Electronic Supplementary Material (ESI) for Dalton Transactions.

Supporting Information

Palladium(0) Complexes of Diferrocenylmercury Diphosphines: Synthesis, X-ray Structure Analyses, Catalytic Isomerization, and C-Cl Bond Activation

*Alain C. Tagne Kuate,[a,b] Roger. A. Lalancette,[a] Dirk Bockfeld,[c] Matthias Tamm,[c] and Frieder Jäkle[a]**

[a] Department of Chemistry, Rutgers University-Newark, 73 Warren Street, Newark, NJ 07102, USA

[b] Department of Chemistry, Faculty of Sciences, University of Dschang, P.O. Box 67, Dschang, Cameroon

[c] Institut für Anorganische und Analytische Chemie, Technische Universität Braunschweig, Hagenring 30, 38106 Braunschweig, Germany

Experimental Methods and Procedures

Materials. $Pd(dba)_2$ was purchased from commercial sources and used without further purification. The synthesis of ligands **1a** and **1b**[1,2] has been previously reported.

General Methods. All reactions were carried out under an atmosphere of dry nitrogen using high vacuum Schlenk-line techniques or an inert-atmosphere glove box (MBraun). Commercial-grade solvents (toluene, hexanes) were purified by a solvent purification system from Innovative Technologies, degassed and stored over sodium-potassium (NaK) alloy prior to use. Dichloromethane and acetonitrile were distilled from CaH_2, degassed and stored under nitrogen atmosphere. 599.7 MHz ^1H NMR, 150.8 MHz $^{13}C\{^1H\}$ NMR, and 202.5 MHz $^{31}P\{^1H\}$ NMR spectra were recorded on a Bruker Avance III HD NMR spectrometer (Bruker BioSpin, Billerica, MA) or a 600 INOVA NMR spectrometer (Varian Inc., Palo Alto, CA) equipped with a 5 mm dual broadband gradient probe (Nalorac, Varian Inc., Martinez, CA). Chemicals shifts (δ) are given in ppm and were referenced internally to deuterated solvents (^{13}C) or to their residual protic signals (^1H) ($CDCl_3$ 7.26 (^1H), 77.36 (^{13}C); C_6D_6 7.15 (^1H), 128.62 (^{13}C)). $^{31}P\{^1H\}$ NMR spectra were referenced externally to H_3PO_4. Coupling constants (J) are reported in Hertz (Hz) and splitting patterns are indicated as s (singlet), d (doublet), t (triplet), pt (pseudo triplet), br (broad), nr (non-resolved), and m (multiplet), and the following abbreviations are used for signal assignments: Ph = phenyl, Cp = cyclopentadienyl, dba = dibenzylidineacetone. High-resolution electrospray ionization-mass spectra (ESI-MS) were obtained on an Apex Ultra 7.0 Hybrid FTMS and MALDI-TOF (time-of-flight) MS data on a Bruker Ultraflextreme. Elemental analyses were performed by Quantitative Technologies Inc., Whitehouse, NJ.

Caution: Organomercury compounds are highly toxic! The use of appropriate non-permeable and resistant gloves is essential.

X-ray diffraction analysis. Reflections for *meso*-**2a** and *meso*-**3a** were collected on a Bruker SMART APEX II CCD Diffractometer using CuKα (1.54178 Å) radiation at 100 K. Data processing, Lorentz-polarization, and face-indexed numerical absorption corrections were performed using SAINT, APEX, and SADABS computer programs.[3-5] The structures were solved by direct methods and refined by full-matrix least squares based on F^2 with all reflections using the SHELXTL V6.14 program package.[6,7] Non-hydrogen atoms were refined with anisotropic displacement coefficients. All H atoms were found in electron-density difference maps and treated as idealized contribution. A crystal of (p*S*p*S*)-**2b** was mounted on a MiTeGen mount with per-fluorinated inert oil. Data were recorded on a Rigaku XtaLAB Synergy S Single Source diffractometer equipped with a PhotonJet Cu-microfocus source and a HyPix-6000HE detector. Data reduction was performed with CrysalisPro.[8] Absorption correction was based on multi-scans and face indexing and integration on a Gaussian grid was applied. The structure was solved by intrinsic phasing with SHELXT-2018/2[6] and refined on F^2 using the program SHELXL-2018/3[6] in OLEX[9]. H atoms were placed in idealized positions and refined using a riding model. Structural data have been deposited with the Cambridge Structure Database as supplementary publications CCDC 2053820-2053822.

All new metal complexes have been fully characterized by ^{1}H, $^{13}C\{^{1}H\}$, $^{31}P\{^{1}H\}$ NMR spectroscopy, high-resolution mass spectrometry (MALDI-TOF or ESI-MS) showing ion peaks for loss of the labile dba ligand (compounds **2**) or loss of a chloride ion (compounds **3**), and single crystal X-ray diffraction. A representative elemental analysis of compound **2b** is provided as well.

Synthesis of Bis(*ortho*-diphenylphosphinoferrocenyl)mercury Palladium(0) Dibenzylideneacetone Complex 2a (*meso*). To a solution of bis(dibenzylideneacetone)palladium(0) ($Pd(dba)_2$, 7.7 mg, 0.0134 mmol) in anhydrous toluene (2 mL) was added slowly a solution of *meso*-**1a** (14.1 mg, 0.0150 mmol) in toluene (2 mL) at room temperature. The color of the solution turned immediately red. The mixture was stirred for 0.5h and the solvent evaporated under reduced pressure. The ^{31}P NMR spectrum of the crude product showed full conversion into a new species. The residue was washed several times with hexanes, separated by decantation, and dried under vacuum to afford **2a** as a red solid. Yield: 14.0 mg (82%). X-ray quality crystals were obtained by slow partial evaporation of a solution of the compound in C_6H_6/decane. ^1H NMR (599.7 MHz, C_6D_6, 25 °C): δ = 8.20 (m, 4H, *o*-Ph), 7.73 (d, $^3J_{H,H}$ = 16.2 Hz, 2H, dba), 7.48 (m, 4H, *o*-Ph'), 7.20 (br m, 4H, dba), 7.14 (m, 4H, *m*-Ph), 7.09 (br m, 2H, dba), 7.02 (br m, 4H, dba), 6.85 (m, 6H, *m*-Ph' + *p*-Ph), 6.82 (d, $^3J_{H,H}$ = 15.6 Hz, 2H, dba), 4.41 pt ($^3J_{H,H}$ = 2.4 Hz, 2H, Cp), 4.38 (br m, 2H, Cp), 4.33 (br m, 2H, Cp), 4.19 (s, 10H, free Cp). $^{13}C\{^1H\}$ NMR (150.8 MHz, C_6D_6, 25 °C): δ = 188.1 (CO, dba), 142.7 (br s, CH-dba), 141.1 (pt, $^{1,3}J_{C,P}$ = 16.4 Hz, *i*-Ph), 138.6 (pt, $^{1,3}J_{C,P}$ = 17.9 Hz, *i*-Ph'), 136.9 (pt, $^{2,4}J_{C,P}$ = 9.7 Hz, *o*-Ph), 136.1 (nr, *m*-Ph), 133.3 (pt, $^{2,4}J_{C,P}$ = 7.5 Hz, *o*-Ph'), 130.7 (nr, *m*-Ph'), 130.7 (s, *p*-Ph'), 130.6 (s, *p*-Ph'), 129.6 (s, Ph-dba), 129.2 (s, Ph-dba), 128.9 (s, Ph-dba), 126.4 (br s, CH-dba), 125.3 (br, Ph-dba), 111.2 (pt, $^{2,4}J_{C,P}$ = 25.4 Hz, *i*-Cp–Hg), 85.4 (pt, $^{1,3}J_{C,P}$ = 24.1 Hz, *i*-Cp–P), 78.8 (pt, $^{2,4}J_{C,P}$ = 11.0 Hz, Cp), 75.4 (nr, Cp), 74.4 (nr, Cp), 69.8 (s, free Cp). $^{31}P\{^1H\}$ NMR (202.5 MHz, C_6D_6, 25 °C): δ = 20.9 (s). High-resolution MALDI-TOF MS (positive mode, anthracene): m/z 1045.9719 ($[M-dba]^+$, 100%, calcd for $^{12}C_{44}{}^1H_{36}{}^{56}Fe_2{}^{200}Hg^{31}P_2{}^{106}Pd$ 1045.9741).

Synthesis of Bis(*ortho*-diphenylphosphinoferrocenyl)mercury Palladium(0) Dibenzylideneacetone Complex 2b (p*S*p*S*). To a solution of

bis(dibenzylideneacetone)palladium(0) ($Pd(dba)_2$, 12.6 mg, 0.0219 mmol) in toluene (2 mL) was added slowly a solution of **1b** (20.5 mg, 0.0218 mmol) in toluene (3 mL) at room temperature. The color of the solution turned immediately red. The mixture was stirred for 0.5 h and the solvent evaporated under reduced pressure. The $^{31}P\{^1H\}$ NMR spectrum of the crude product showed full conversion into a new species. The residue was washed several times with hexanes, separated by decantation, and dried under vacuum to afford (p*S*,p*S*)-**2b** as a red solid. Yield: 24.0 mg (86%). X-ray quality crystals were obtained by slow partial evaporation of a solution of the compound in toluene/decane. ^1H NMR (599.7 MHz, C_6D_6, 25 °C): δ = 8.03 (m, 4H, *o*-Ph), 7.71 (d, $^3J_{H,H}$ = 15.0 Hz, 2H, dba), 7.69 (m, 4H, *m*-Ph), 7.22 (br m, 4H, dba), 7.11 (br m, 6H, *o*,*p*-Ph'), 7.05 (br m, 10H, *m*-Ph' + dba), 6.94 (t, $^3J_{H,H}$ = 7.2 Hz, 2H, *p*-Ph'), 6.76 (d, $^3J_{H,H}$ = 15.6 Hz, 2H, dba), 4.32 (br d, 4H overlapping, Cp), 4.04 (nr, 2H, Cp), 4.02 (s, 10H, free Cp). $^{13}C\{^1H\}$ NMR (150.8 MHz, C_6D_6, 25 °C): δ = 188.3 (CO, dba), 140.5 (br s, CH-dba), 140.5 (pt, $^{1,3}J_{C,P}$ = 15.1 Hz, *i*-Ph), 137.2 (pt, $^{1,3}J_{C,P}$ = 17.5 Hz, *i*-Ph'), 136.4 (nr, *o*-Ph), 136.3 (nr, *m*-Ph), 133.3 (pt, $^{2,4}J_{C,P}$ = 7.5 Hz, *o*-Ph'), 130.6 (nr, *m*-Ph'), 130.4 (s, *p*-Ph'), 129.6 (s, Ph-dba), 129.4 (nr, *p*-Ph'), 129.1 (s, Ph-dba), 128.9 (s, Ph-dba), 126.6 (br s, CH-dba), 124.8 (br s, Ph-dba), 110.1 (pt, $^{2,4}J_{C,P}$ = 22.0 Hz, *i*-Cp–Hg), 85.8 (pt, $^{1,3}J_{C,P}$ = 25.0 Hz, *i*-Cp–P), 79.4 (pt, $^{2,4}J_{C,P}$ = 8.7 Hz, Cp), 74.4 (nr, Cp), 74.2 (nr, Cp), 70.3 (s, free Cp). $^{31}P\{^1H\}$ NMR (202.5 MHz, C_6D_6, 25 °C): δ = 18.1 (s). High-resolution ESI-MS (positive mode, toluene/acetonitrile): 1046.9868 ($[M–dba+H]^+$, 100%, calcd for $^{12}C_{44}{}^1H_{37}{}^{56}Fe_2{}^{200}Hg{}^{31}P_2{}^{106}Pd$ 1046.9819). Elem. Anal. for $C_{44}H_{36}Fe_2HgP_2Pd \cdot C_{17}H_{14}O$: Calcd C 57.25, H 3.94; Found C 57.27, H 3.94.

Competition Reaction of 1a/1b with $Pd(dba)_2$. A solution containing **1a** (10.0 mg, 0.011 mmol) and **1b** (10.0 g, 0.011 mmol) in C_6D_6 (0.7 mL) was added slowly to solution of bis(dibenzylideneacetone)palladium(0), $Pd(dba)_2$ (6.1 mg, 0.011 mmol) in $CDCl_3$ (0.3 mL) at

room temperature. The mixture was introduced into an NMR tube and the reaction followed by ^{31}P NMR spectroscopy. After 0.5 h standing at room temperature: $^{31}P\{^{1}H\}$ NMR (202.5 MHz, $CDCl_3$, 25 °C): δ = −13.3 (8%), −12.6 (32%), 17.6 (46%), 21.5 (14%).

Dichloromethane Activation: Synthesis of Bis(*ortho*-diphenylphosphinoferrocenyl)-mercury Palladium(II) Complex 3a (*meso*). 2a (6.6 mg, 5.15 μmol) was dissolved in CH_2Cl_2 (0.9 mL). No change of color was observed upon mixing. The solution was stirred at 40 °C for 24 h. A progressive change of color from red to yellow-orange was observed. The mixture was allowed to cool to room temperature and all volatiles were removed under high vacuum. Analysis of the crude product by ^{31}P NMR revealed almost full conversion into a new species. The residue was washed several times with hexanes and recrystallized from CH_2Cl_2/hexanes by slow partial evaporation at room temperature to give **3a** as a yellow-orange crystalline solid. Yield 5.4 mg (93%). ^{1}H NMR (599.7, MHz, $CDCl_3$, 25 °C): δ = 8.48 (m, 4H, *o*-Ph), 7.61 (br m, 5H, *m,p*-Ph), 7.18 (br m, 1H, *p*-Ph), 7.12 (m, 4H, *m*-Ph'), 6.97 (m, 4H, o-Ph'), 4.66 (pt, $^{3}J_{H,H}$ = 1.7 Hz, 2H, Cp), 4.60 (nr, 2H, Cp), 4.56 (nr , 2H, Cp), 4.12 (s, 10H, free Cp), 2.15 (t, $^{2}J_{P,H}$ = 9.6 Hz, 2H, CH_2Cl). $^{13}C\{^{1}H\}$ NMR (150.8 MHz, $CDCl_3$, 25 °C): δ = 136.8 (pt, $^{2,4}J_{P,C}$ = 6.0 Hz, o-Ph), 136.1 (pt, $^{1,3}J_{C,P}$ = 22.6 Hz, *i*-Ph), 133.8 (pt, $^{1,3}J_{C,P}$ = 24.1 Hz, *i*-Ph'), 132.9 (nr, *o*-Ph'), 131.0 (s, *p*-Ph), 129.4 (s, *p*-Ph'), 128.2 (pt, $^{3,5}J_{P,C}$ = 6.0 Hz *m*-Ph), 127.7 (pt, $^{3,5}J_{P,C}$ = 4.5 Hz *m*-Ph'), 113.6 (pt, $^{1,3}J_{C,P}$ = 19.6 Hz, *i*-Cp–Hg), 81.3 (pt, $^{1,3}J_{C,P}$ = 28.7 Hz, *i*-Cp–P), 77.2 (nr, Cp), 75.5 (nr, Cp), 73.6 (nr, Cp), 70.8 (s, free Cp), 43.2 (s, CH_2Cl). $^{31}P\{^{1}H\}$ NMR (202.5 MHz, $CDCl_3$, 25 °C): δ = 25.1 (s). High-resolution ESI-MS (positive mode, CH_2Cl_2/acetonitrile): m/z 1094.9316 ($[M-Cl]^+$, 100%, calcd for $^{12}C_{45}{}^{1}H_{38}{}^{35}Cl^{56}Fe_2{}^{200}Hg^{31}P_2{}^{106}Pd$ 1094.9578), 1080.9441 ($[M-CH_2Cl]^+$, 45%, calcd for $^{12}C_{44}{}^{1}H_{36}{}^{35}Cl^{56}Fe_2{}^{200}Hg^{31}P_2{}^{106}Pd$ 1080.9421).

Dichloromethane Activation: Synthesis of Bis(*ortho*-diphenylphosphinoferrocenyl)-mercury Palladium(II) Complex 3b (p*S*p*S*). 2b (pSpS, 30.0 mg, 0.0234 mmol) was dissolved in CH_2Cl_2 (0.7 mL). No change of color was observed upon mixing. The solution was stirred at 40 °C for 24 h. A progressive change of color from red to light green was observed. The mixture was allowed to cool to room temperature and all volatiles were removed under high vacuum. Analysis of the crude product by ^{31}P NMR revealed almost full conversion into a new species. The residue was washed three times with hexanes to give **3b** as a yellow solid with a slight greenish tint. Yield 20.0 mg (75%). All attempts to obtain single crystals of **3b** for X-ray structures analyses furnished amorphous solids. ^{1}H NMR (599.7, MHz, $CDCl_3$, 25 °C): δ = 8.34 (br m, 2H, *o*-Ph), 8.24 (pt, $^{3}J_{HH}$ = 7.2 Hz, 2H, *o*-Ph), 7.58 (br m, 2H, *o*-Ph'), 7.51 (br m, 3H, m+*p*-Ph), 7.42 (br m, 3H, *o*+*p*-Ph'), 7.31 (br m, 3H, *m*-Ph+*p*-Ph'), 7.26 (br, 1H, *p*-Ph'), 7.20 (pt, $^{3}J_{HH}$ = 7.2 Hz, 2H, *m*-Ph'), 7.12 (pt, $^{3}J_{HH}$ = 7.2 Hz, 2H, *m*-Ph') 4.90 (nr, 1H, Cp), 4.71 (nr, 1H, Cp), 4.64 (nr, 2H, Cp), 4.59 (nr, 1H, Cp), 4.53 (nr, 1H, Cp), 4.24 (s, 5H, free Cp), 4.00 (s, 5H, free Cp), 3.02 (br m, 1H, CH_2Cl), 2.93 (br m, 1H, CH_2Cl). $^{13}C\{^{1}H\}$ NMR (150.8 MHz, $CDCl_3$, 25 °C): δ = 136.7 (nr, *o*-Ph), 136.6 (nr, *o*-Ph), 136.2 (nr, *i*-Ph), 136.0 (nr, *i*-Ph), 134.9 (nr, *i*-Ph'), 134.7 (nr, *i*-Ph'), 133.9 (nr, *o*-Ph), 133.8 (nr, *o*-Ph), 133.7 (nr, *o*-Ph'), 133.6 (nr, *o*-Ph'), 133.2 (nr, *o*-Ph'), 133.1 (nr, *o*-Ph'), 130.9 (nr, *m*-Ph), 130.2 (nr, *m*-Ph), 129.7 (nr, m-Ph), 129.4 (nr, m-Ph), 128.3 (nr, m-Ph'), 128.2 (nr, m-Ph'), 127.8 (s, *p*-Ph), 127.8 (s, *p*-Ph), 127.7 (s, *p*-Ph'), 127.6 (s, *p*-Ph'), 112.3 (d, $^{2}J_{P,C}$ = 37.7 Hz, *i*-Cp-Hg), 108.6 (nr, $^{2}J_{P,C}$ = 37.7 Hz, *i*-Cp'-Hg), 81.5 (d, $^{2}J_{P,C}$ = 45.2 Hz, *i*-Cp'-P), 79.0 (nr, Cp), 78.9 (nr, Cp), 78.6 (d, $^{2}J_{P,C}$ = 53.0 Hz, *i*-Cp'-P), 76.6 (nr, Cp), 75.2 (nr, Cp'), 75.0 (nr, Cp'), 73.4 (nr, Cp'), 70.8 (s, free Cp), 70.2 (s, free Cp'), 39.9 (s, CH_2Cl). $^{31}P\{^{1}H\}$ NMR (202.5 MHz, $CDCl_3$, 25 °C): δ = 24.6 (d, $^{2}J_{P,P}$ = 405 Hz), 20.7 (d, $^{2}J_{P,P}$ = 405 Hz). High-resolution ESI-MS (positive

mode, CH_2Cl_2/acetonitrile): m/z 1094.9320 ($[M-Cl]^+$, 100%, calcd for $^{12}C_{45}{}^{1}H_{38}{}^{35}Cl^{56}Fe_2{}^{200}Hg^{31}P_2{}^{106}Pd$ 1094.9578).

Kinetic Study of the CH_2Cl_2 Activation Reaction with 2a/2b. A solution containing a mixture of CH_2Cl_2 (0.4 mL), C_6D_6 (0.6 mL), **2a** (2.1 mg, 0.0016 mmol) and **2b** (2.1 mg, 0.0016 mmol) was introduced into an NMR tube and the reaction followed by ^{31}P NMR spectroscopy at 40 °C. The NMR spectra were recorded every 40 minutes for a total of 400 min.

Table S1. Crystal data and refinement details for **2a**, **2b**, and **3a**.

Compound	**2a** (*meso*)	**2b** (p*S*p*S*)	**3a** (*meso*)
CCDC	**2053820**	**2053821**	**2053822**
empirical formula	$C_{122}H_{94}Fe_4Hg_2O_2P_4Pd_2$	$C_{61}H_{50}Fe_2HgOP_2Pd$	$C_{45}H_{38}Cl_2Fe_2HgP_2Pd \cdot 2\ CH_2Cl_2$
MW	2553.23	1279.64	1300.13
T, K	100	100	100
wavelength, Å	1.54178	1.54184	1.54178
crystal system	Triclinic	Monoclinic	Monoclinic
space group	*P*-1	$P2_1$	$P2_1/c$
a, Å	10.2020(11)	9.5692(1)	11.975(4)
b, Å	12.6346(13)	12.8337(2)	27.776(9)
c, Å	19.684(2)	20.1024(3)	14.345(4)
α, deg	82.830(3)	90	90
β, deg	85.254(3)	91.986(1)	105.223(9)
γ, deg	71.562(3)	90	90
V, Å^3	2385.7(4)	2467.26(6)	4604(2)
Z	1	2	4
ρ_{calc}, g cm^{-3}	1.777	1.722	1.876
μ (Cu Kα), mm^{-1}	14.38	13.91	18.02
crystal size, mm	0.18×0.11×0.07	0.17×0.01×0.01	0.40×0.05×0.04
θ range, deg	2.3–68.7	2.2–77.8	3.2–68.8
limiting indices	–12 ⩽ h ⩽ 12 –11 ⩽ k ⩽ 15 –22 ⩽ l ⩽ 23	–8 ⩽ h ⩽ 11 –16 ⩽ k ⩽ 16 –25 ⩽ l ⩽ 25	–14 ⩽ h ⩽ 12 –32 ⩽ k ⩽ 32 –16 ⩽ l ⩽ 17
reflns collected	18344	44271	42767
independent reflns	7717 [*R*(int) = 0.065]	10288 [*R*(int) = 0.045]	8230 [*R*(int) = 0.049]
data/restraints/parameters	7717/54/650	10288/1/613	8230/12/542
goodness-of-fit on F^2	0.99	1.13	1.02
final *R* indices, [I >2σ(I)] [a]	*R1* = 0.065 w*R2* = 0.173	*R1* = 0.036 *wR2* = 0.102	*R1* = 0.038 w*R2* = 0.082
R indices (all data) [a]	*R1* = 0.1167	*R1* = 0.048	*R1* = 0.051
peak$_{max}$/hole$_{min}$ (e Å^{-3})	2.28 / –3.25	1.15 / -2.50	1.53 / –1.71
Flack parameter		0.015(6)	

[a] $R1 = \Sigma||F_o|-|F_c||/\Sigma|F_o|$; $wR2 = \{\Sigma[w(F_o^2-F_c^2)^2]/\Sigma[w(F_o^2)^2]\}^{1/2}$

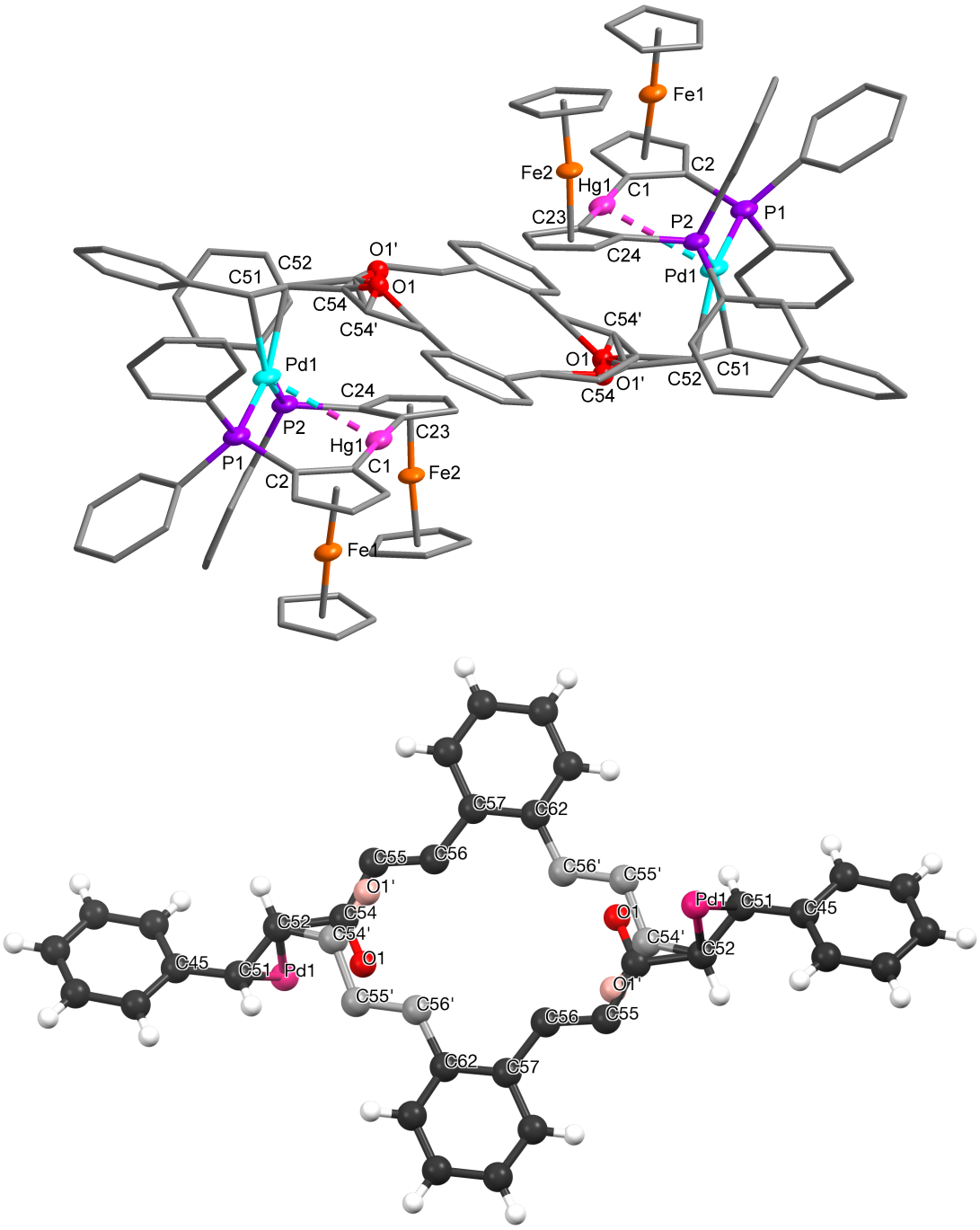

Figure S1. Illustration of two molecules of **2a** (*meso*) showing the disorder of the dba ligand.

Analysis of Buried Volume and Ligand Steric Maps

We examined the diphosphine ligands in complexes **2a** and **2b** by performing an analysis of the buried volume using the Samb*V*ca program.[10] As expected we find a very large percentage of buried volume (% V_{bur}) for the diphosphine ligand in both LPd^0(dba) complexes, larger than that of most common diphosphines[11]. Using a sphere of 5.0 Å to account for the large size of the dba ligand and the steric pressure of the diferrocenylmercury unit relatively far from the Pd, the V_{bur} of the ligand in the *meso*-isomer **2a** of 57.3% is in fact slightly smaller than that of the *pSpS*-isomer **2b** of 62.5% (the differences for a 3.5 Å sphere with % V_{bur} of 58.2% and 61.0% respectively are even smaller). A similar trend is seen for the respective *trans*-coordinated $LPdCl_2$ complexes, for which the % V_{bur} within a 3.5 Å sphere of the *meso*-isomer of 61.0 % is smaller to that of *pSpS*-isomer of 63.1%. Clearly, the steric hindrance exerted by the diphosphines cannot be described simply by the volume they take up. However, the dramatic differences between the ligands are evident in the respective steric maps (Figure 3). In **2a** the coparallel diferrocene unit forces the Ph groups away from the proligand backbone but leaving space above the diferrocene unit. On the other hand, for **2b**, the diferrocene backbone arrangement does not provide space close to the backbone for a ligand as large as the dba ligand.

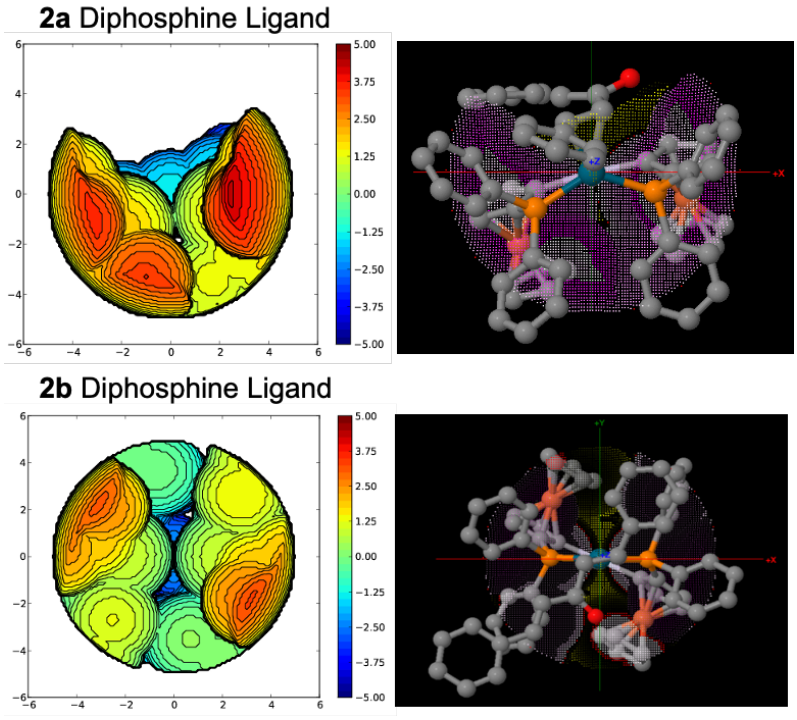

Figure S2. Steric maps for the diphosphines in the Pd^0 complexes **2a** (top) and **2b** (bottom).

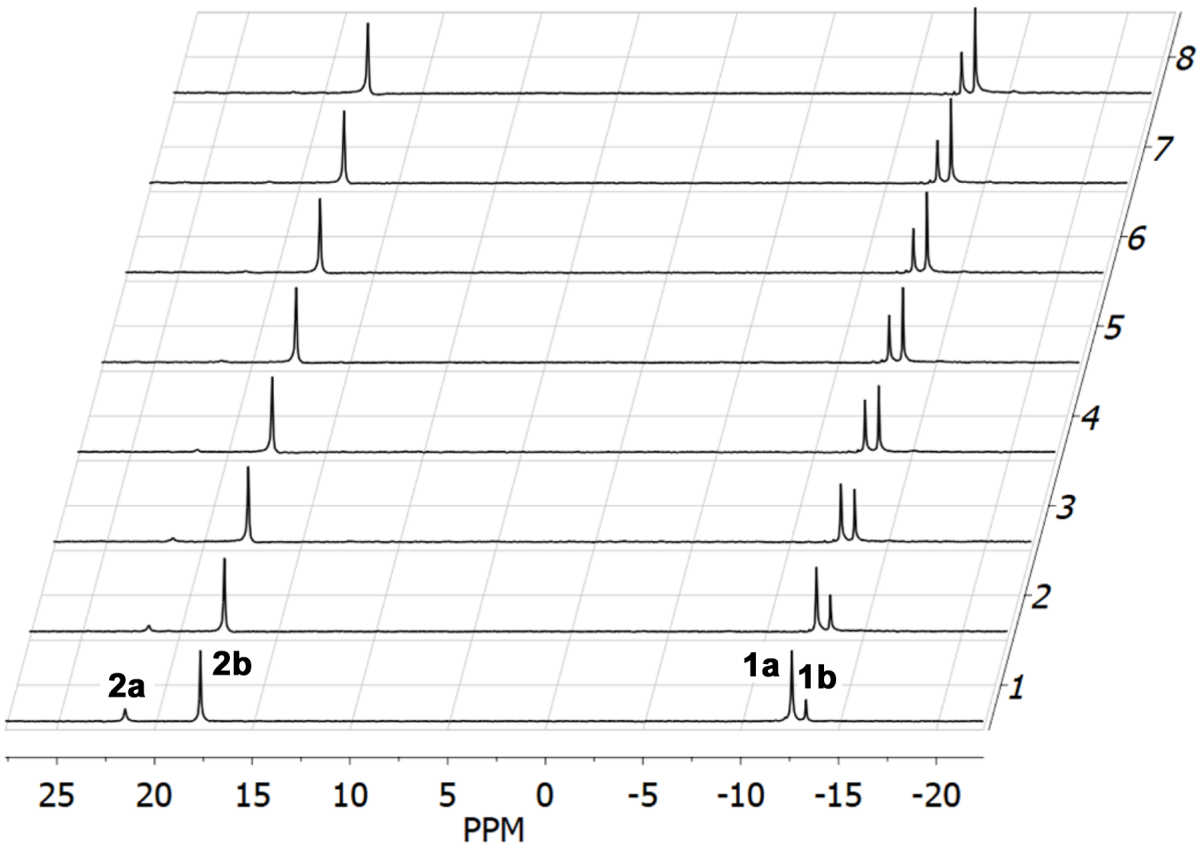

Figure S3a. 202.5 MHz $^{31}P\{^{1}H\}$ NMR spectra for the competitive reaction between **1a**/**1b** and $Pd(dba)_2$ in C_6D_6; the spectra were recorded every 30 min.

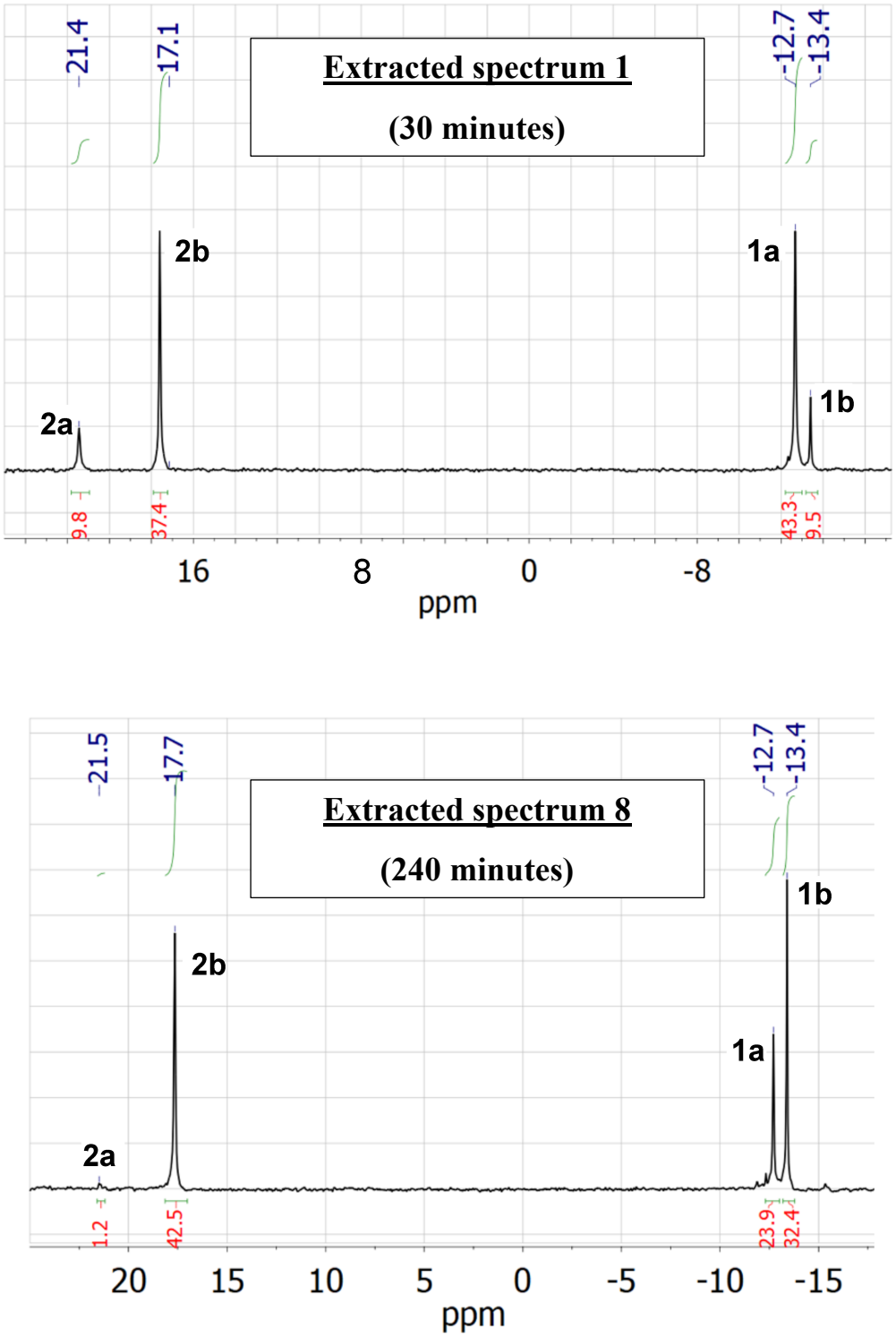

Figure S3b. Extracted 202.5 MHz $^{31}P\{^{1}H\}$ NMR spectra 1 (top) and 8 (bottom) for the competitive reaction between **1a**/**1b** and $Pd(dba)_2$ in C_6D_6.

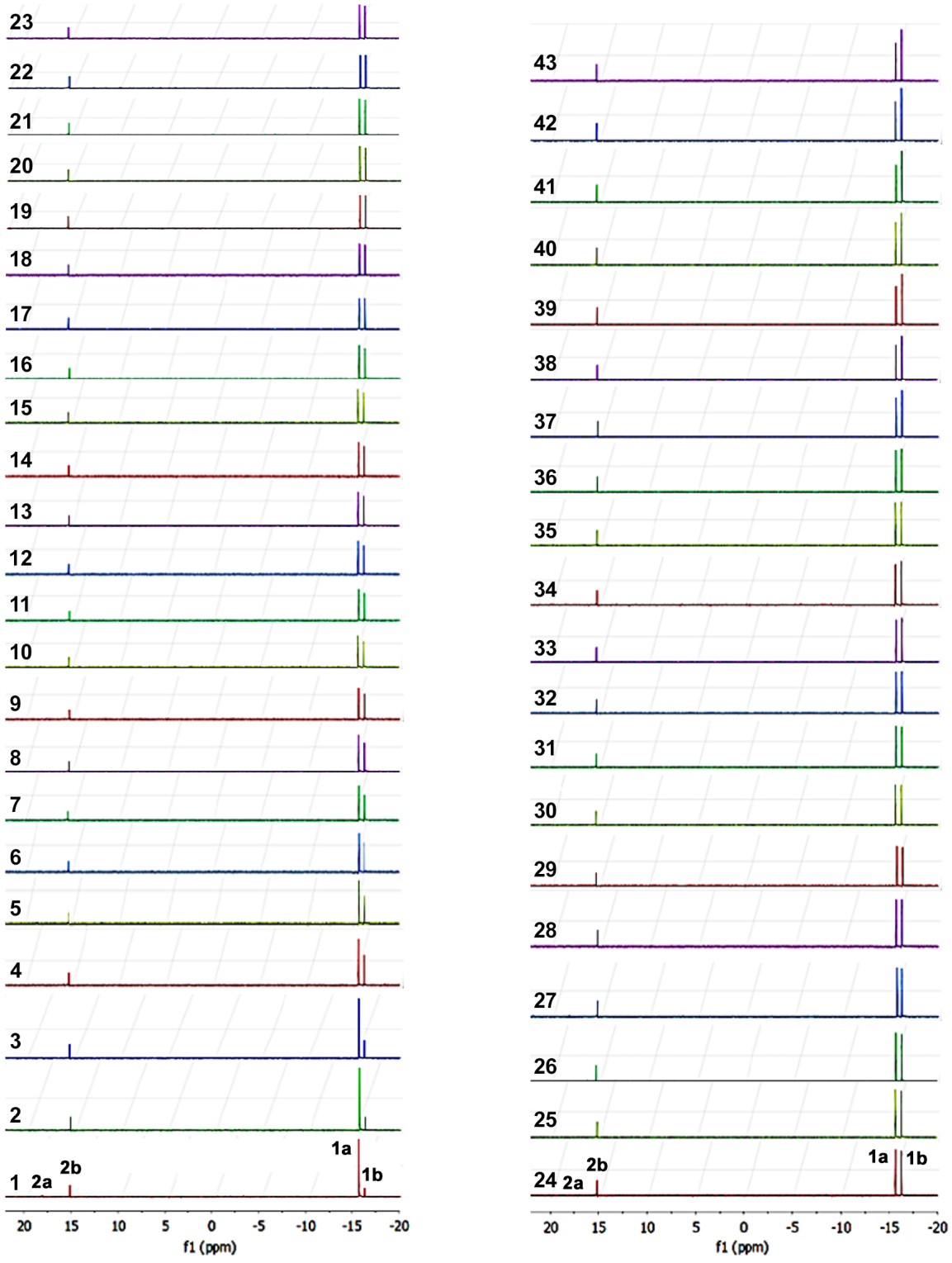

Figure S4. 202.5 MHz $^{31}P\{^{1}H\}$ NMR spectra for the interconversion of *meso*-**1a** into *rac*-**1b** catalyzed by $Pd(dba)_2$ (ca. 15 mol%) in C_6D_6 (initial ratio of *meso*-**1a** : *rac*-**1b** at 84% : 16%; time between measurements 40 minutes.

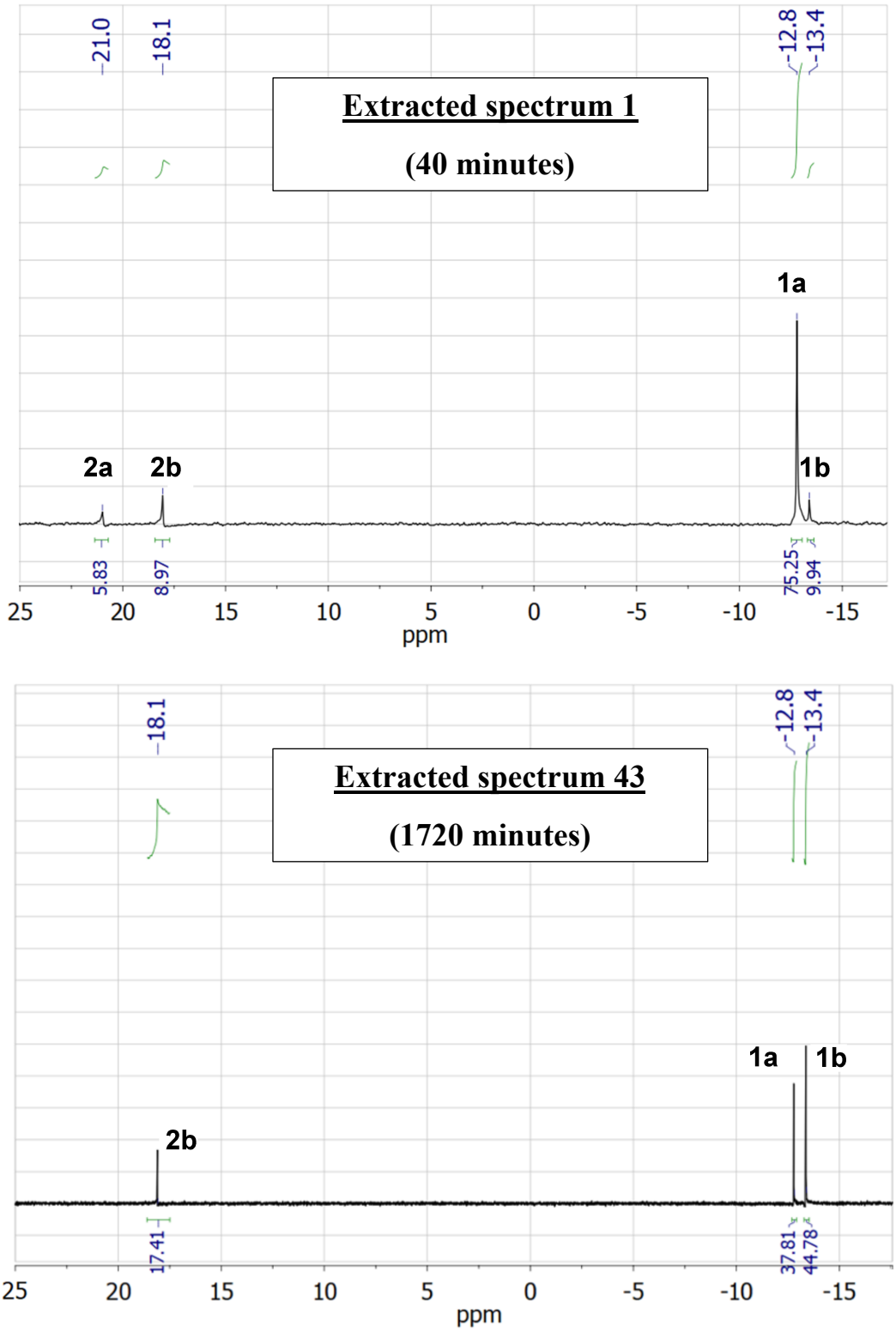

Figure S5. Extracted 202.5 MHz $^{31}P\{^{1}H\}$ NMR spectra 1 (top) and 43 (bottom) for the catalytic interconversion of *meso*-**1a** into *rac*-**1b** catalyzed by $Pd(dba)_2$ (ca. 15 mol%).

Spectral Data for Isolated Compounds

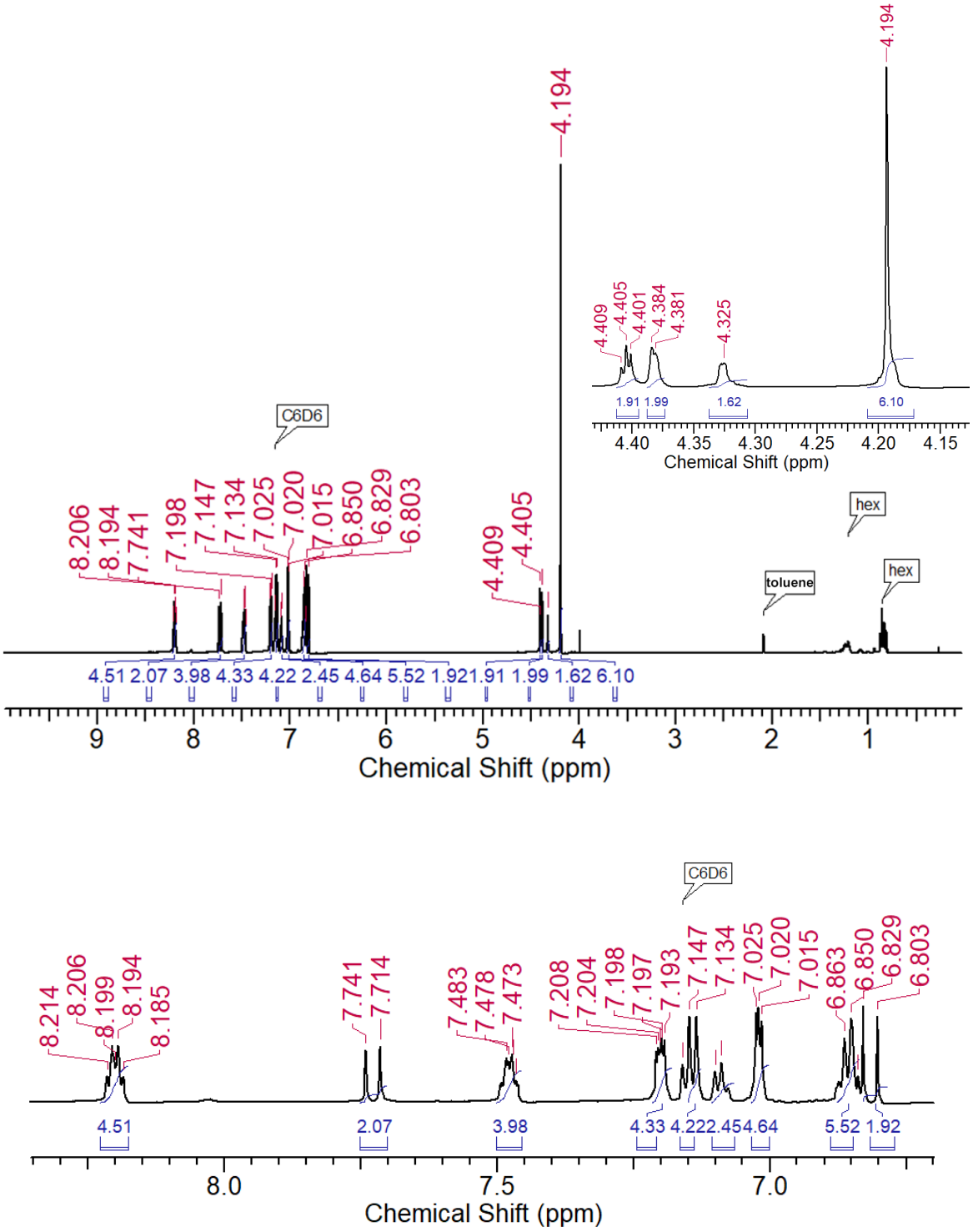

Figure S6. 599.7 MHz ^{1}H NMR spectrum and expansions of **2a** (meso) in C_6D_6.

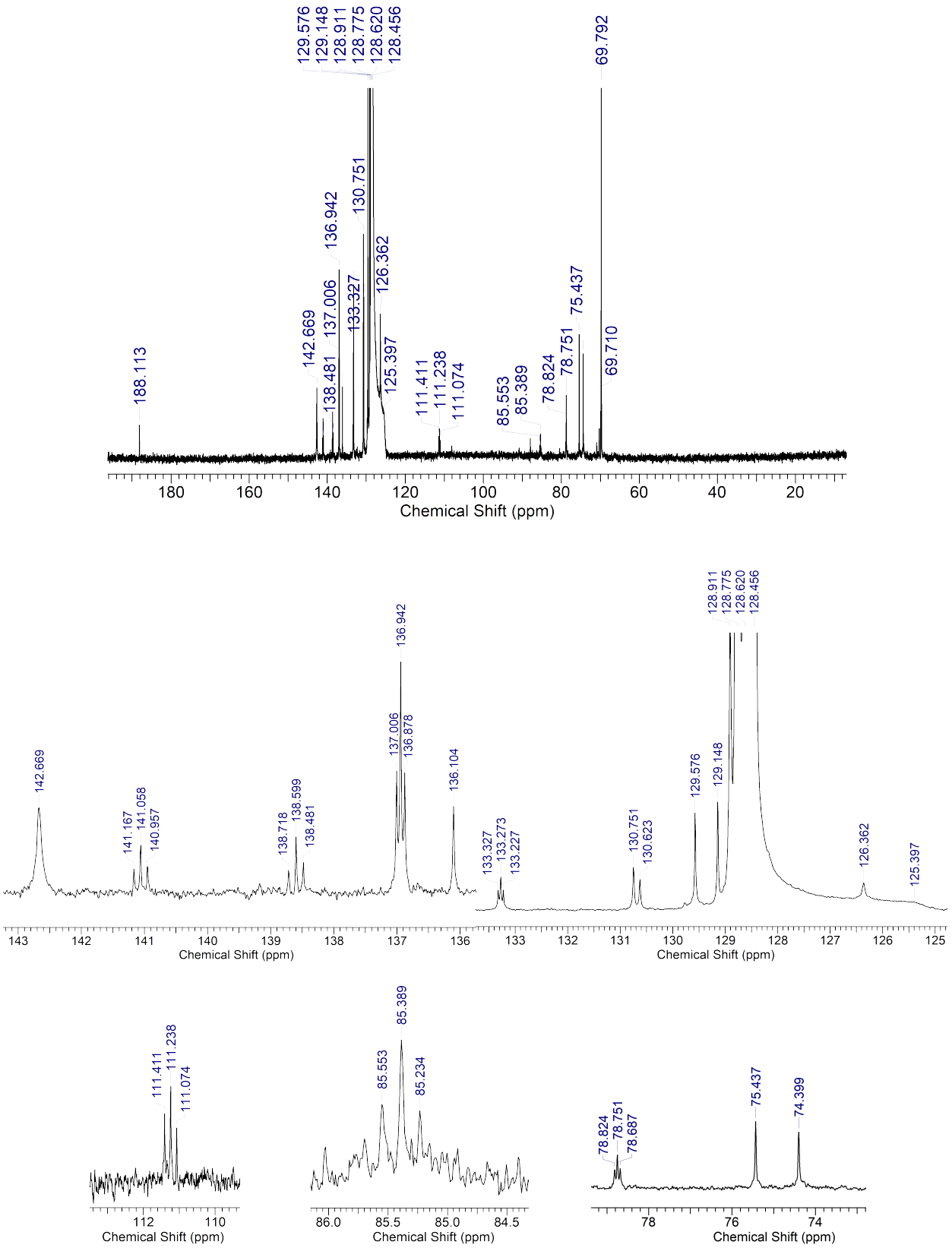

Figure S7. 150.8 MHz $^{13}C\{^{1}H\}$ NMR spectrum and expansions of **2a** (meso) in C_6D_6.

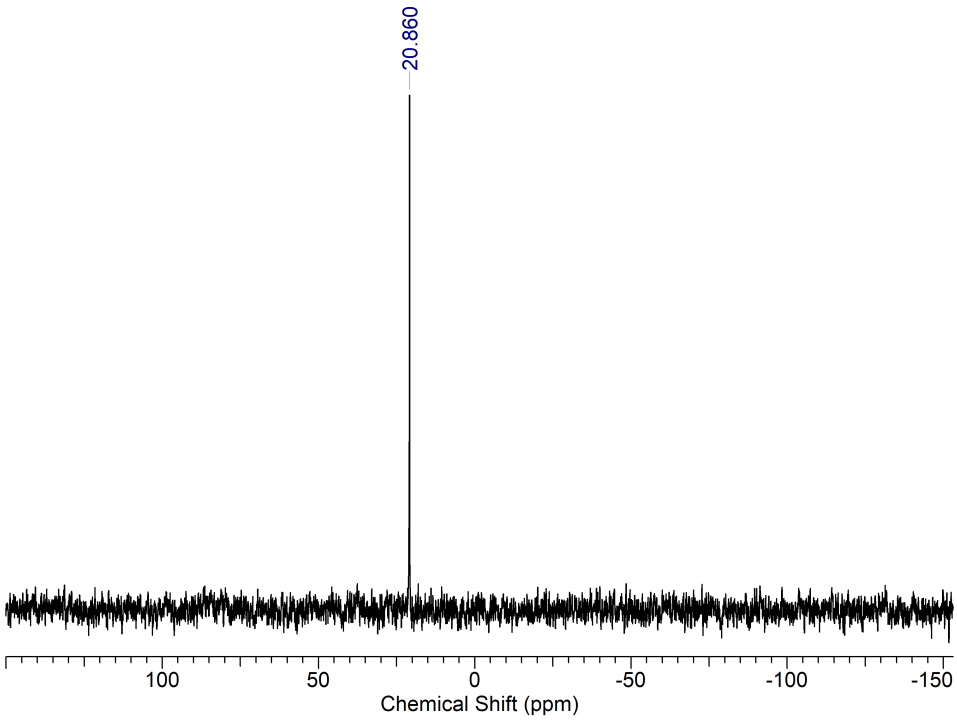

Figure S8. 202.5 MHz $^{31}P\{^{1}H\}$ NMR spectrum of **2a** (*meso*) in C_6D_6.

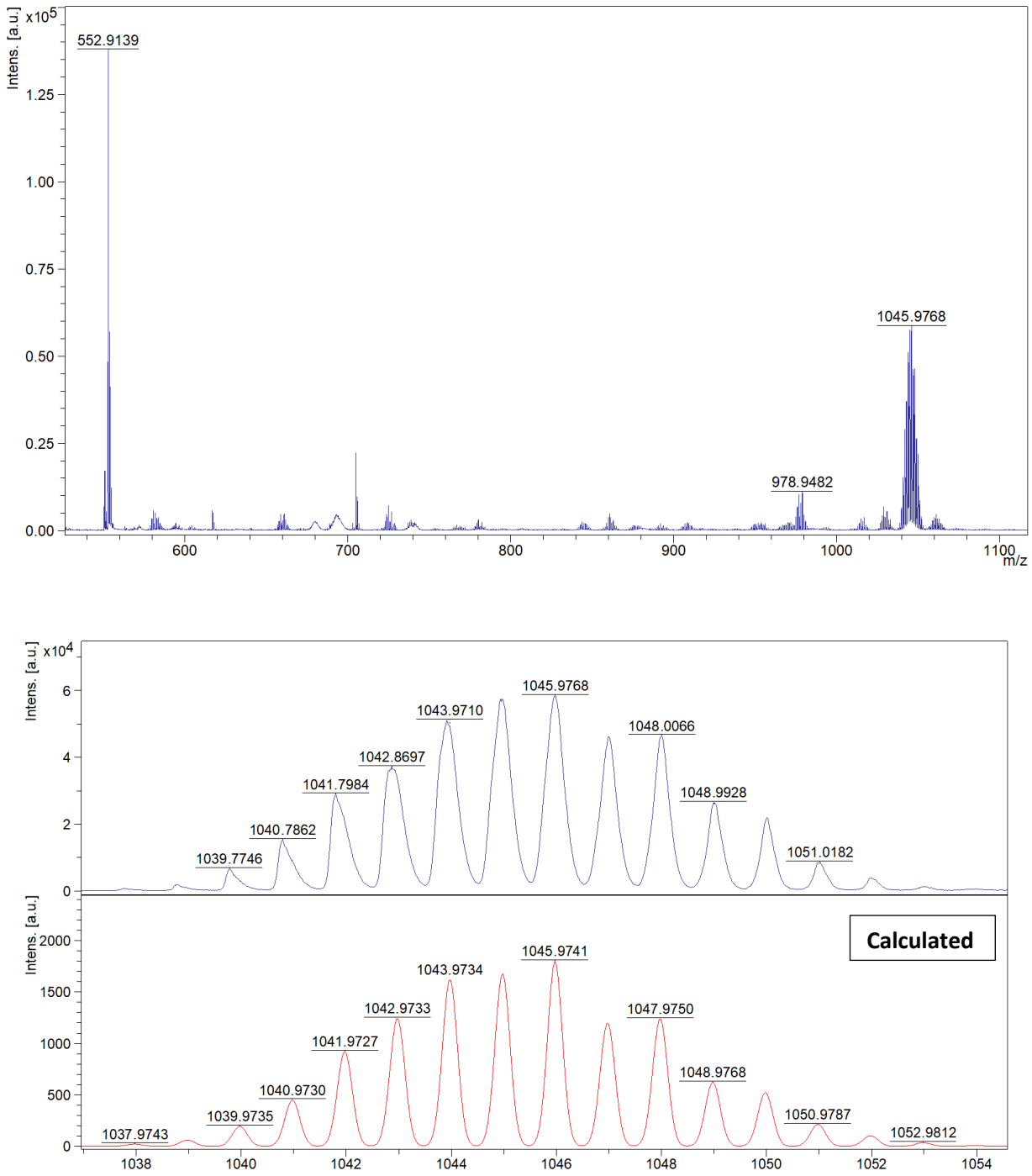

Figure S9. MALDI-TOF MS spectrum of **2a** (meso) and expansion.

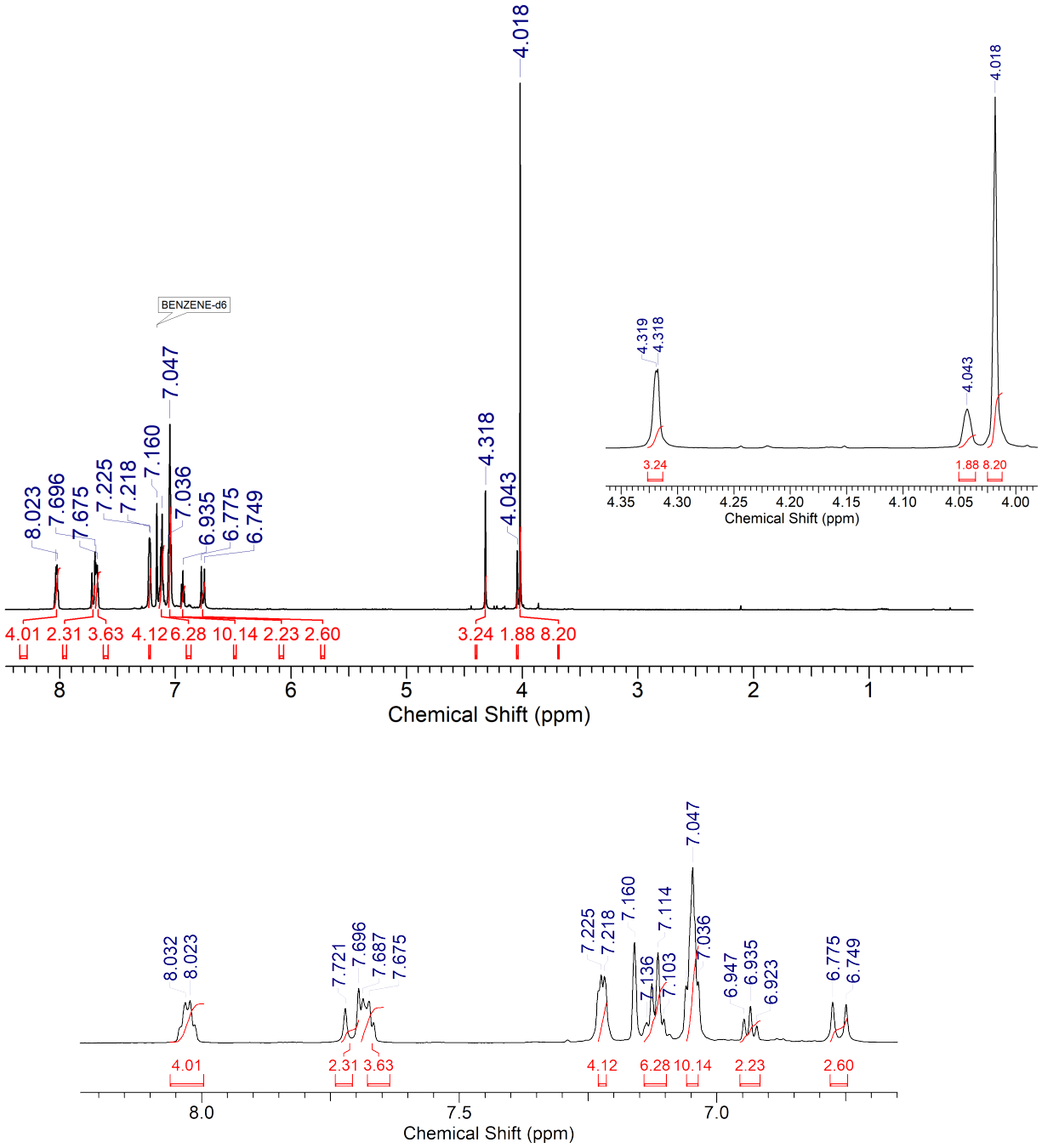

Figure S10. 599.7 MHz ^{1}H NMR spectrum and expansions of **2b** (p*S*p*S*) in C_6D_6.

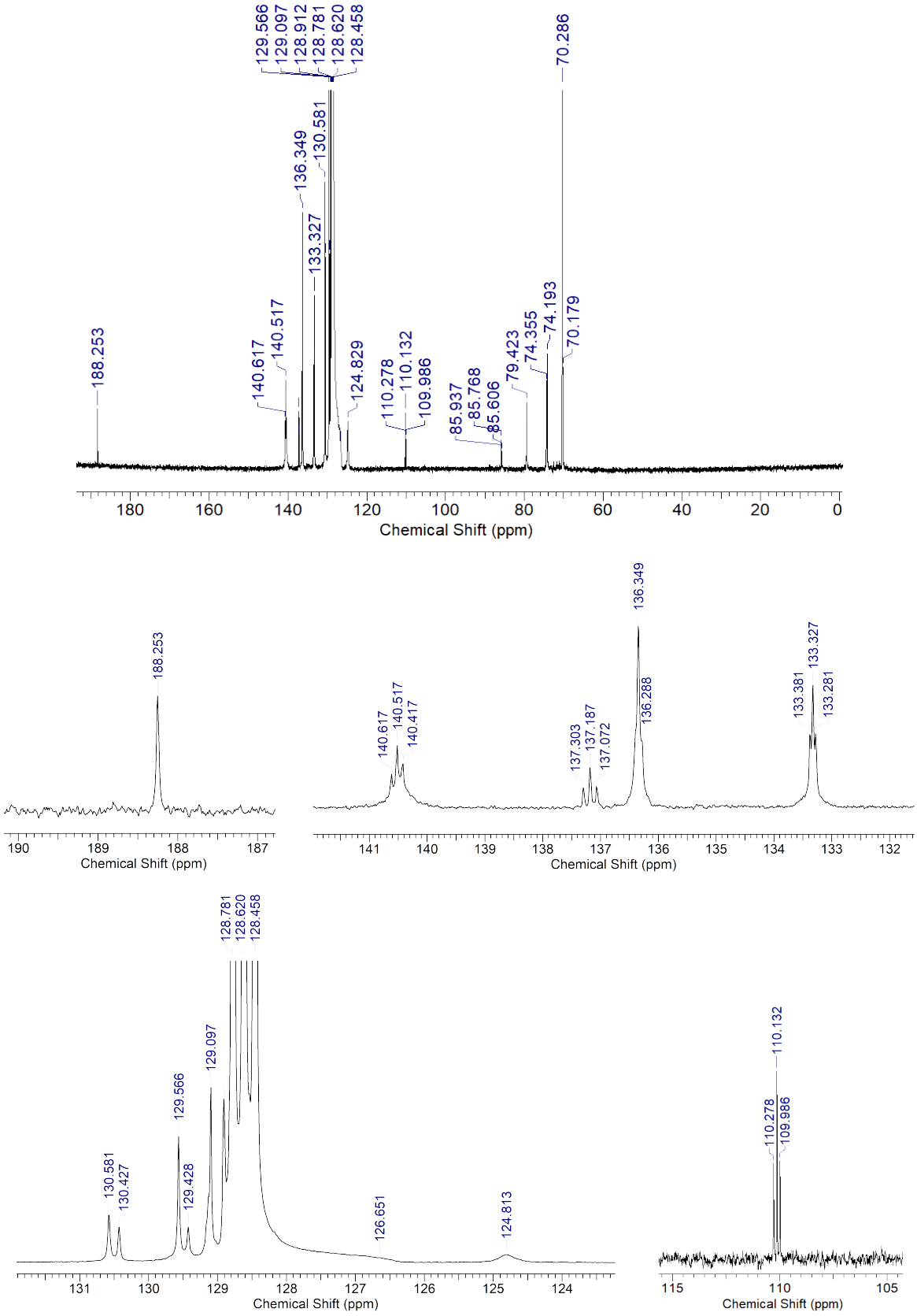

Figure S11. 150.8 MHz $^{13}C\{^{1}H\}$ NMR spectrum and expansions of **2b** (p*S*p*S*) in C_6D_6.

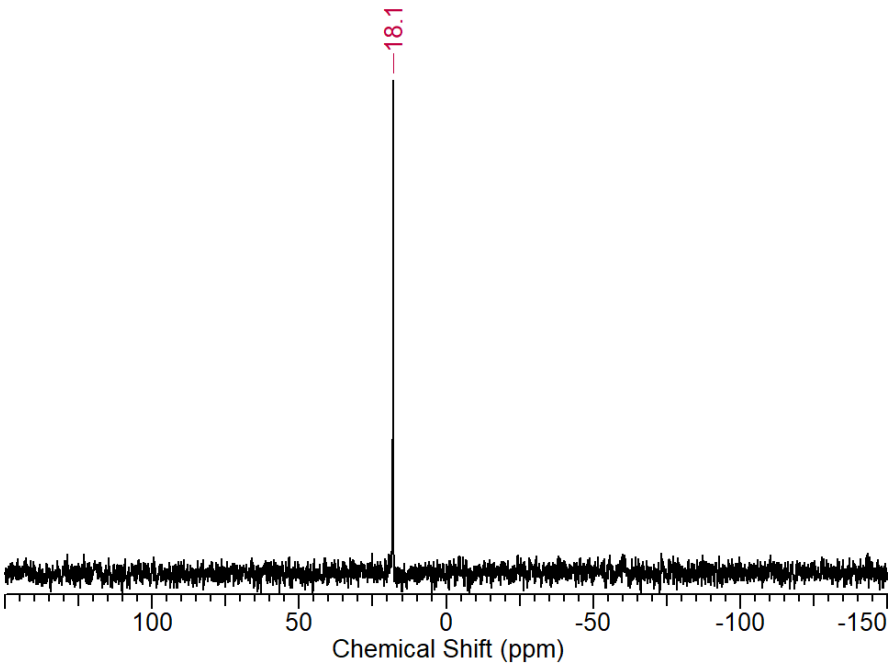

Figure S12. 202.5 MHz $^{31}P\{^{1}H\}$ NMR spectrum of **2b** (p*S*p*S*) in C_6D_6.

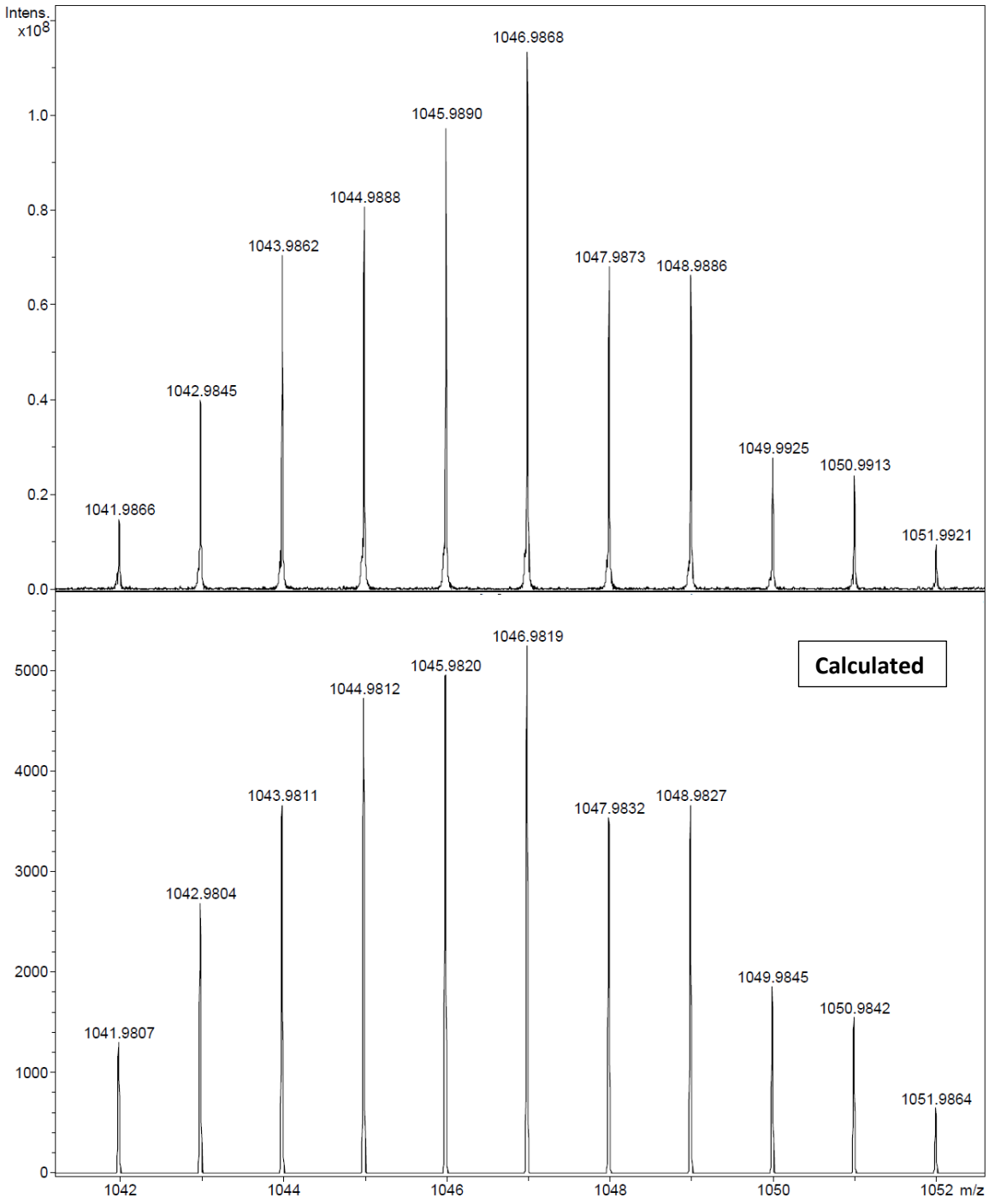

Figure S13. Expansion of ESI-MS (positive mode) spectrum of **2b** in toluene/CH_3CN.

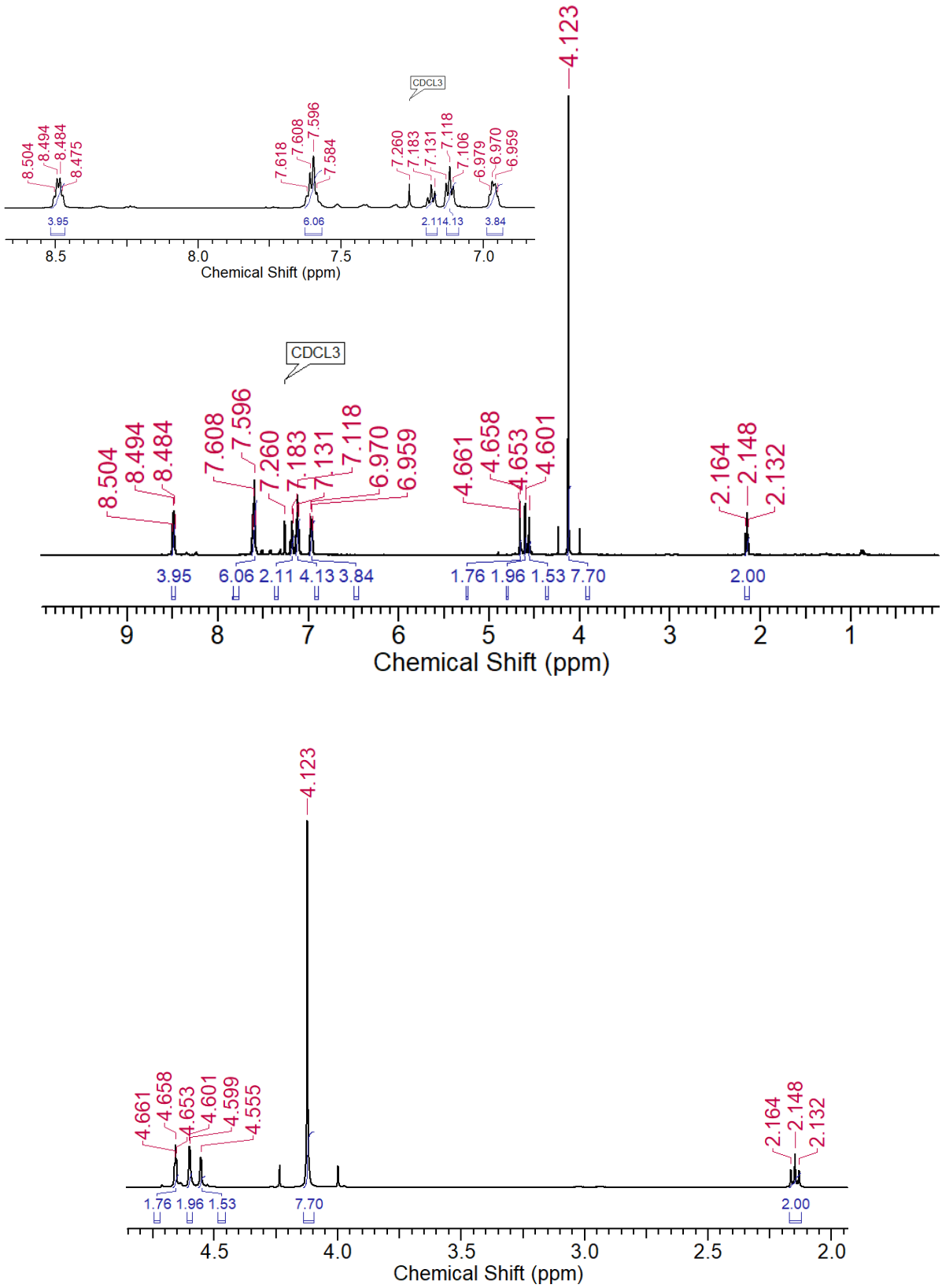

Figure S14. 599.7 MHz ^{1}H NMR spectrum and expansions of **3a** (meso) in $CDCl_3$.

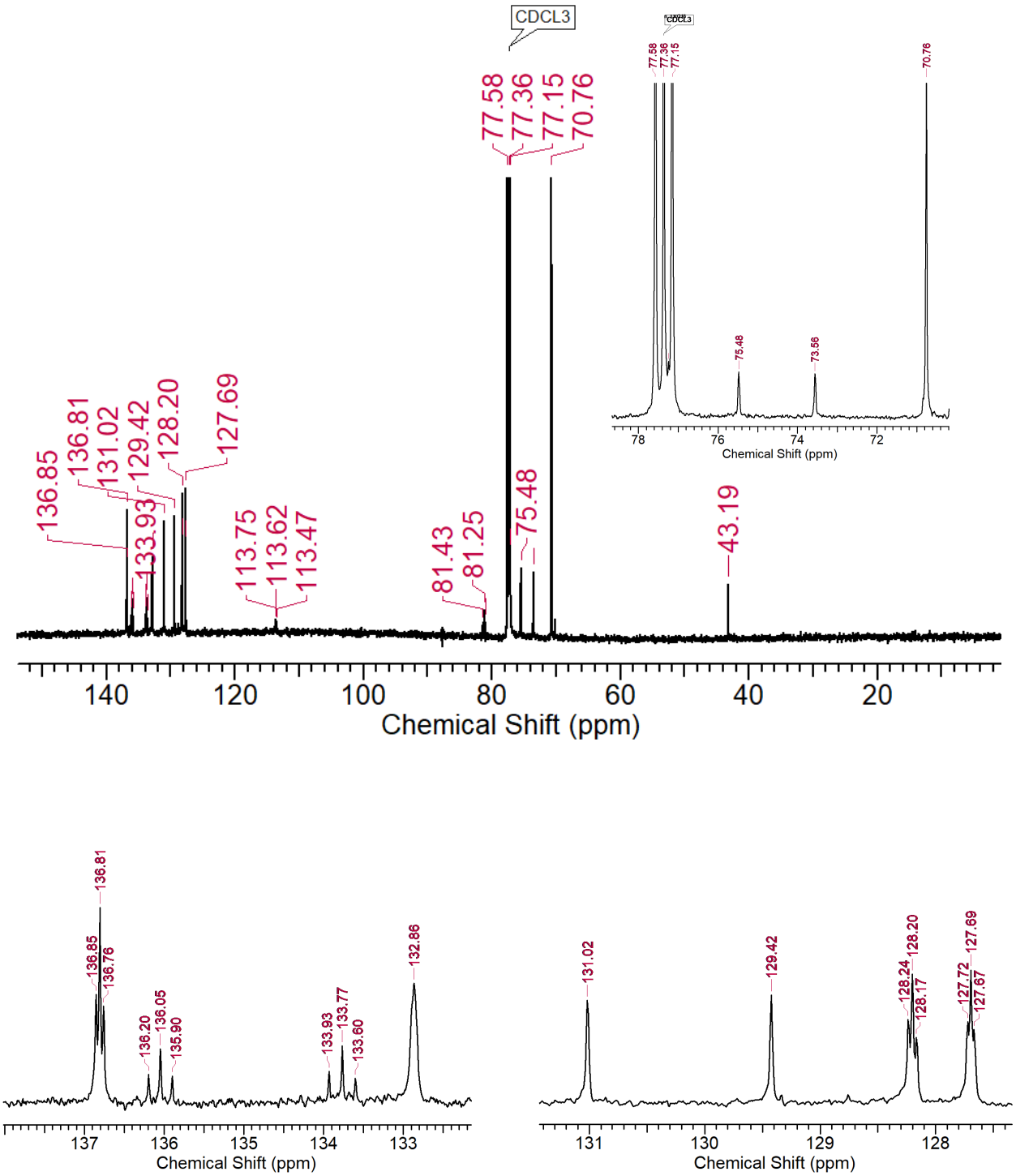
CDCL3
77.58
77.36
77.15
70.76
136.85
136.81
131.02
129.42
128.20
127.69
133.93
113.75
113.62
113.47
81.43
81.25
75.48
43.19
140
120
100
80
60
40
20
Chemical Shift (ppm)
78
76
74
72
Chemical Shift (ppm)
75.48
73.56
136.81
136.85
136.76
136.20
136.05
135.90
133.93
133.77
133.60
132.86
137
136
135
134
133
Chemical Shift (ppm)
131.02
129.42
128.24
128.20
128.17
127.72
127.69
127.67
131
130
129
128
Chemical Shift (ppm)

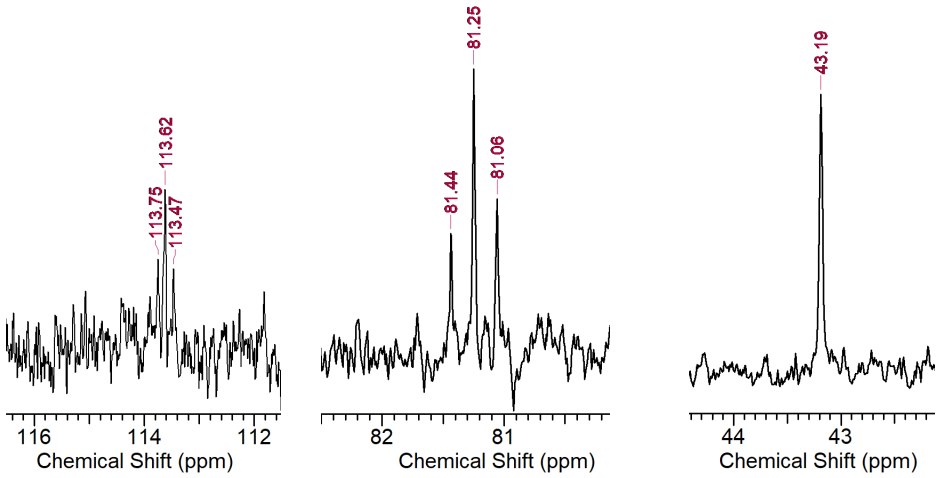

Figure S15. 150.8 MHz $^{13}C\{^{1}H\}$ NMR spectrum and expansions of **3a** (meso) in $CDCl_3$.

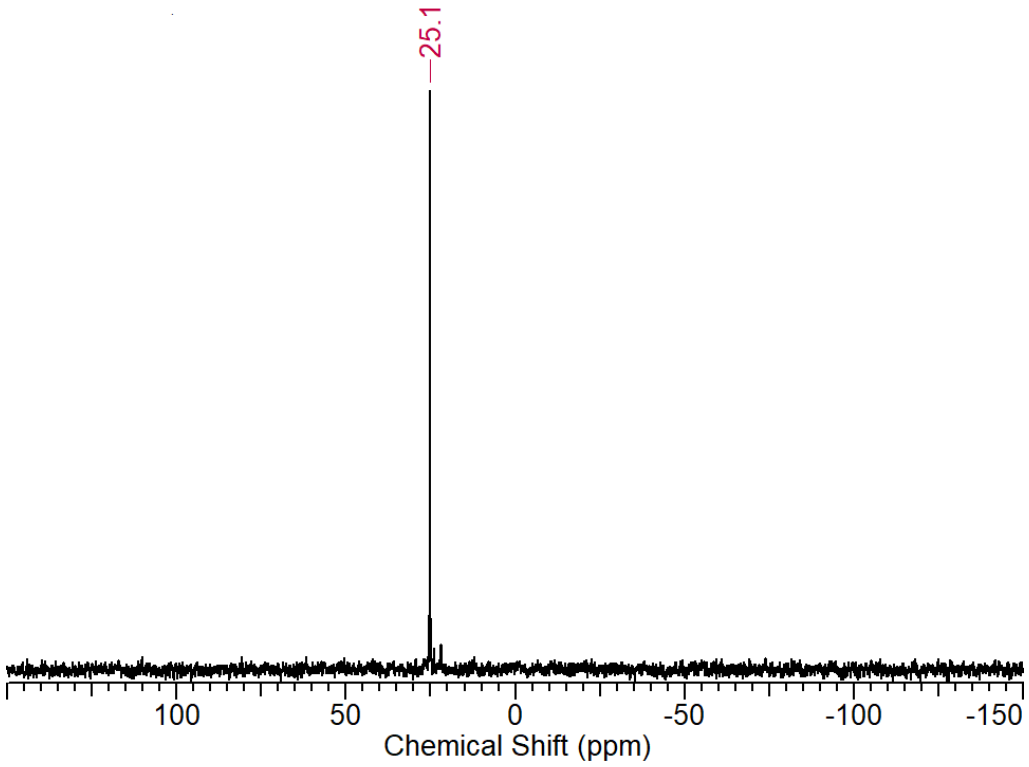

Figure S16. 202.5 MHz $^{31}P\{^{1}H\}$ NMR spectrum of **3a** in $CDCl_3$.

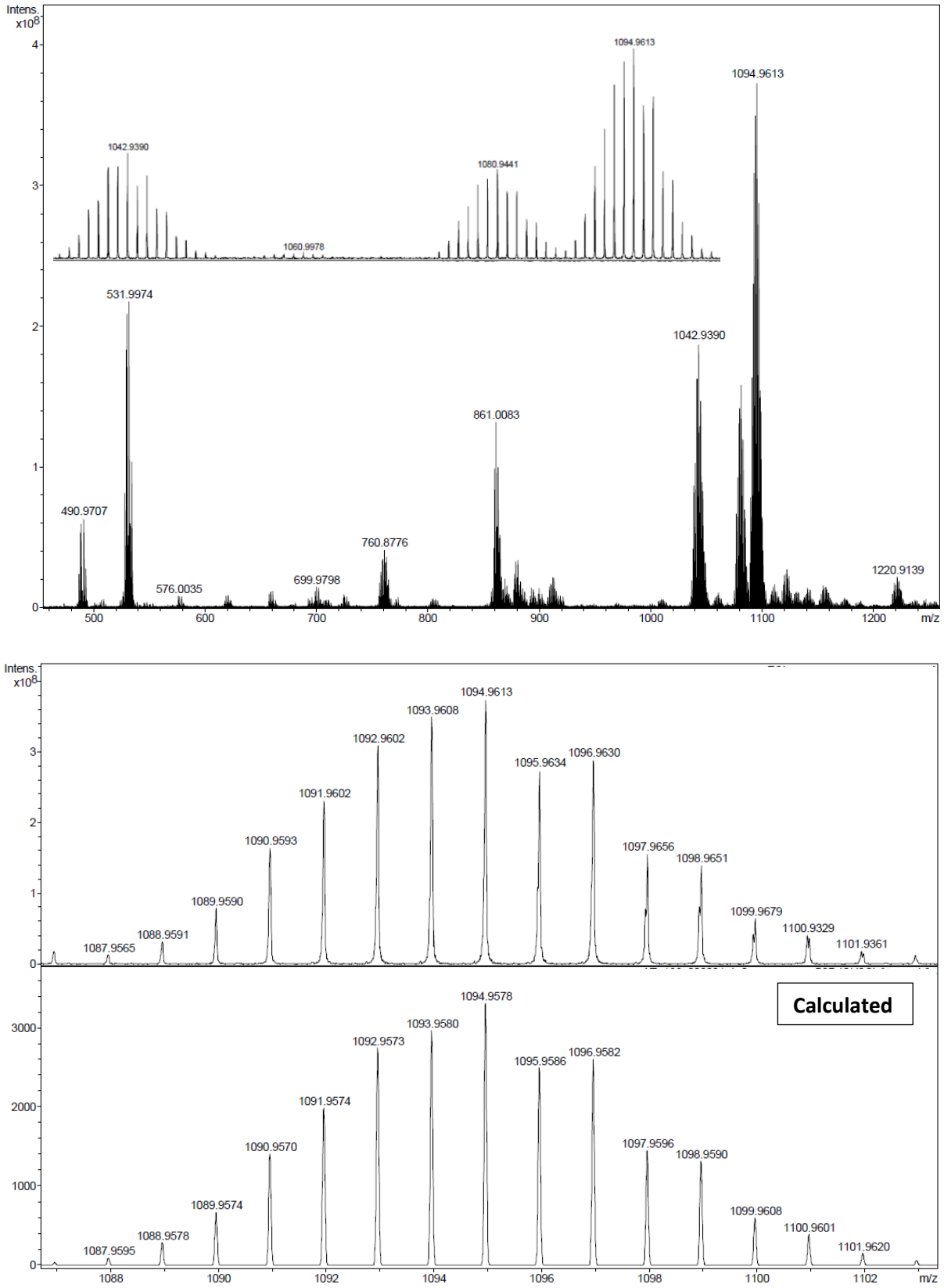

Figure S17. ESI-MS spectrum and expansions of **3a** (meso) in CH_2Cl_2/CH_3CN.

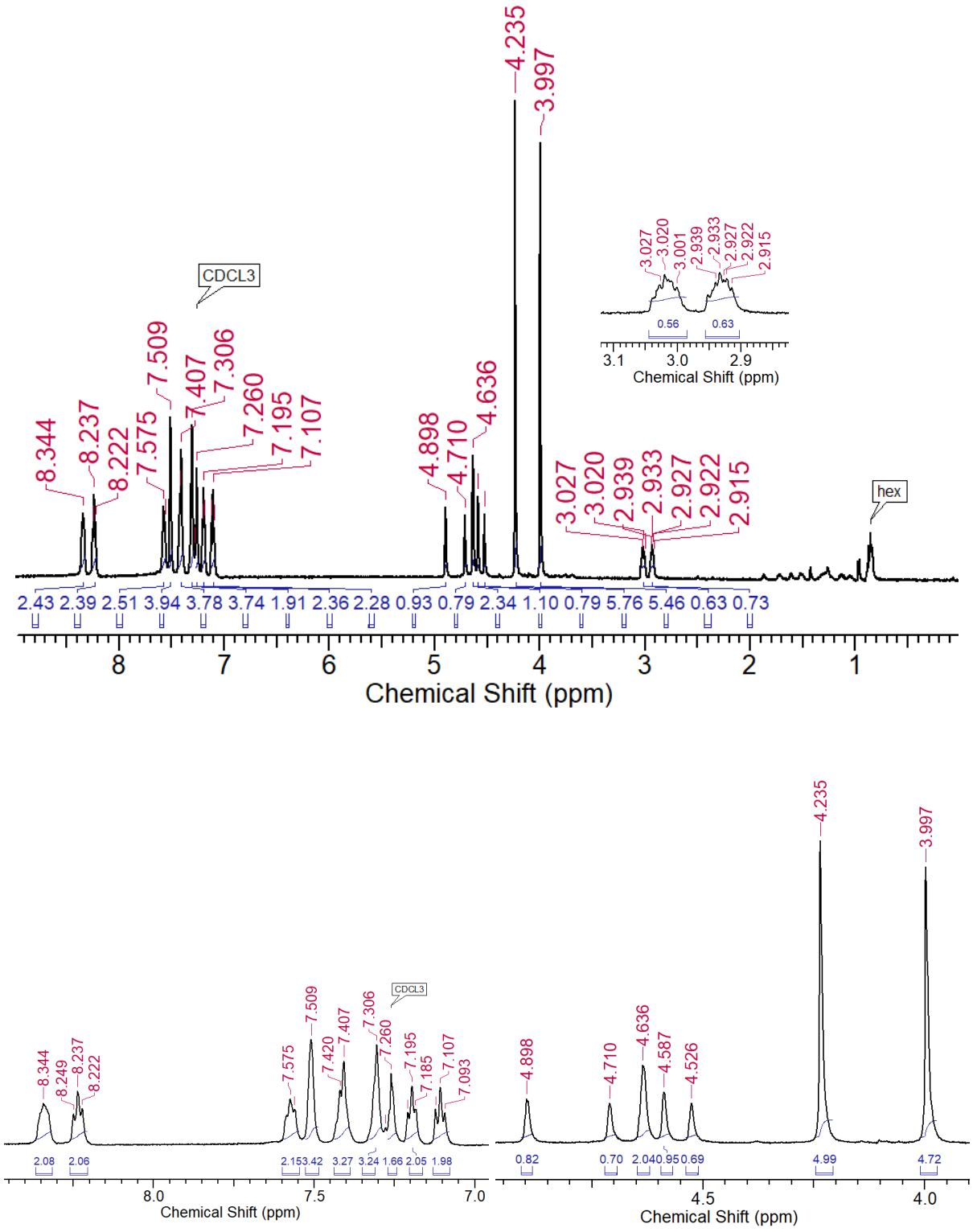

Figure S18. 599.7 MHz ^{1}H NMR spectrum and expansions of **3b** (pSpS) in $CDCl_3$.

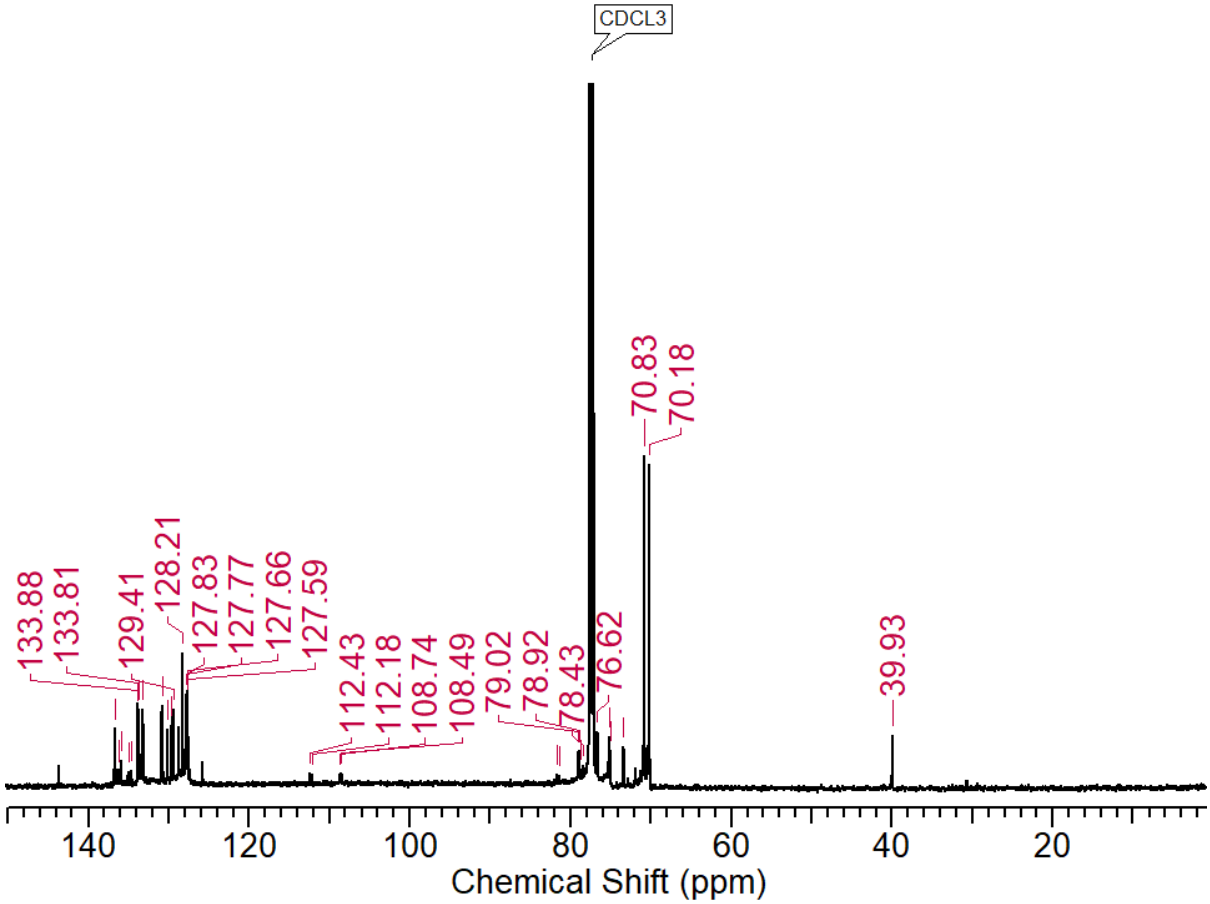
CDCL3
133.88
133.81
129.41
128.21
127.83
127.77
127.66
127.59
112.43
112.18
108.74
108.49
79.02
78.92
78.43
76.62
70.83
70.18
39.93
140
120
100
80
60
40
20
Chemical Shift (ppm)

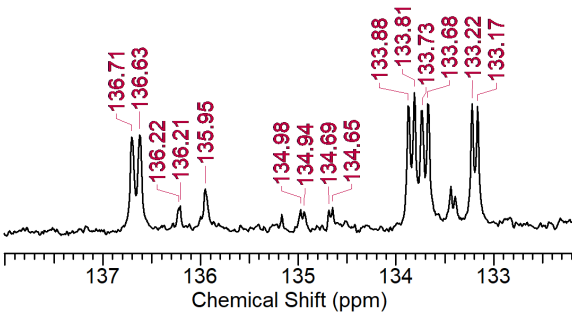
136.71
136.63
136.22
136.21
135.95
134.98
134.94
134.69
134.65
133.88
133.81
133.73
133.68
133.22
133.17
137
136
135
134
133
Chemical Shift (ppm)

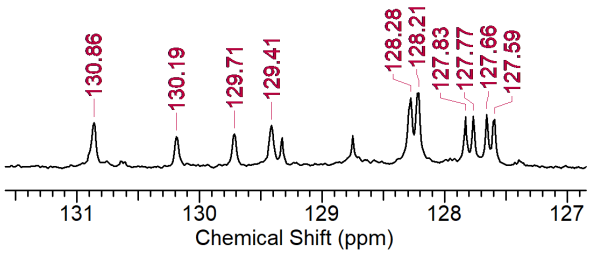
130.86
130.19
129.71
129.41
128.28
128.21
127.83
127.77
127.66
127.59
131
130
129
128
127
Chemical Shift (ppm)

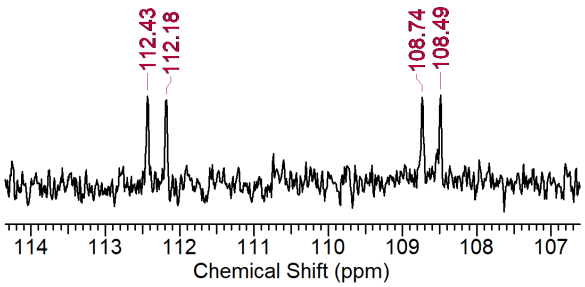
112.43
112.18
108.74
108.49
114
113
112
111
110
109
108
107
Chemical Shift (ppm)

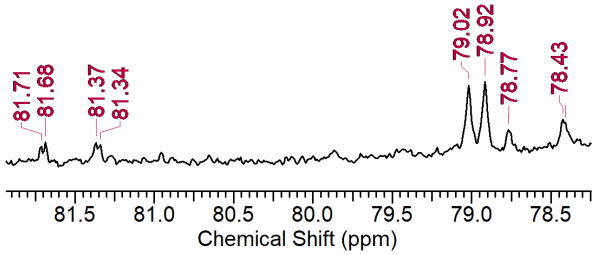
81.71
81.68
81.37
81.34
79.02
78.92
78.77
78.43
81.5
81.0
80.5
80.0
79.5
79.0
78.5
Chemical Shift (ppm)

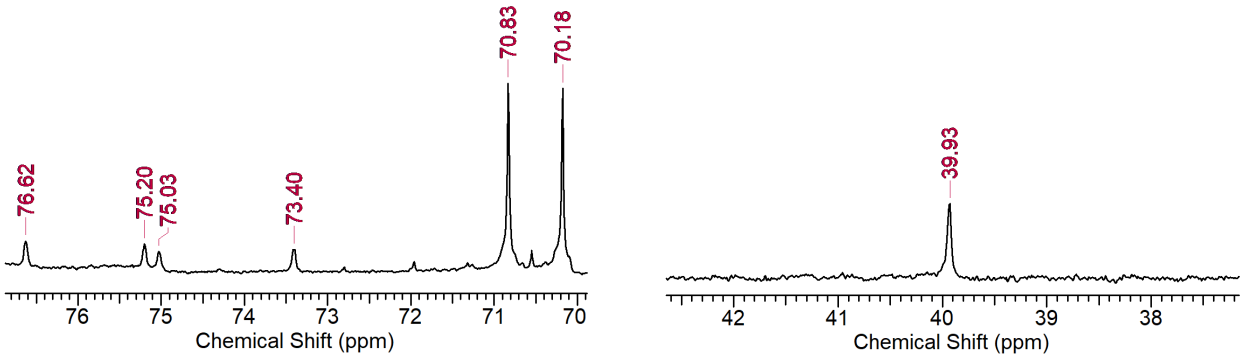

Figure S19. Expansions of the 150.8 MHz $^{13}C\{^{1}H\}$ NMR spectrum of **3b** (pSpS) in $CDCl_3$.

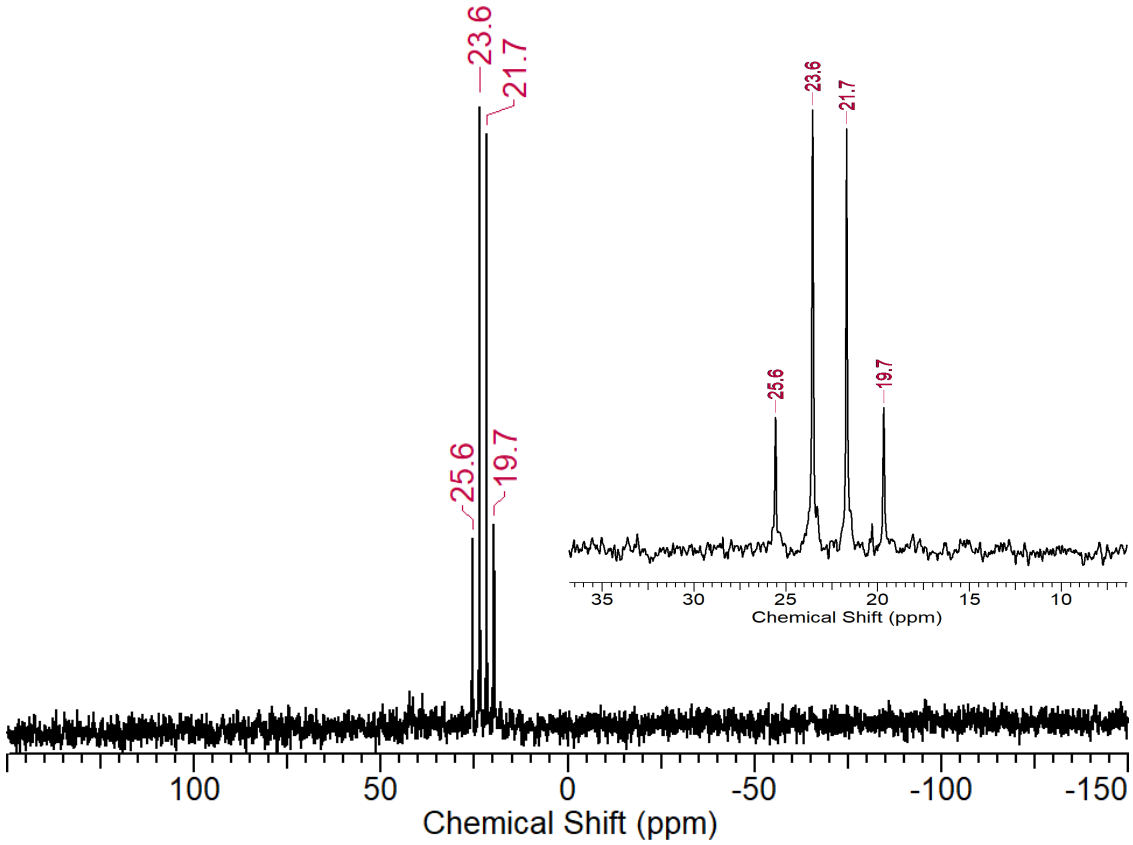

Figure S20. 202.5 MHz $^{31}P\{^{1}H\}$ NMR spectrum and expansion of **3b** (pSpS) in $CDCl_3$.

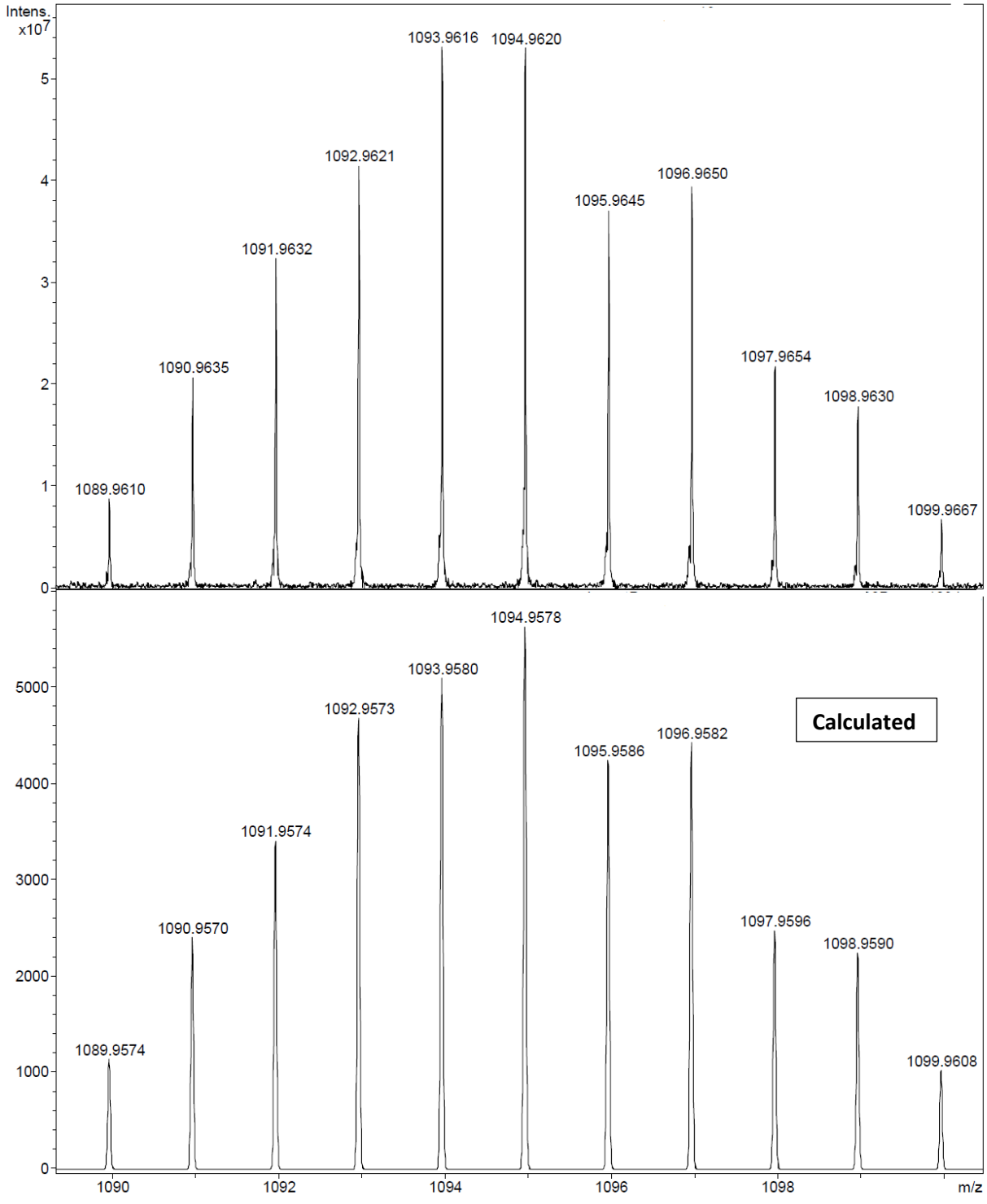

Figure S21. ESI-MS spectrum and expansion of **3b** (pSpS) in CH_2Cl_2/acetonitrile.

References

1. A. C. Tagne Kuate, R. A. Lalancette, T. Bannenberg, M. Tamm, F. Jäkle, *Dalton Trans*., 2019, **48**, 13430-13439.
2. A. C. Tagne Kuate, R. A. Lalancette, T. Bannenberg, F. Jäkle, *Angew. Chem. Int. Ed*. 2018, **57**, 6552-6556.
3. Bruker (2005). *SAINT* Version 7.23a. Bruker AXS Inc., Madison, Wisconsin, USA.
4. Bruker (2006). *APEX 2* Version 2.0-2. Bruker AXS Inc., Madison, Wisconsin, USA.
5. G. M. Sheldrick (2008). SADABS. University of Göttingen, Germany.
6. G. M. Sheldrick, *Acta Cryst.*, 2008, **A64**, 112-122.
7. G. M. Sheldrick, SHELXL, *Acta Cryst.*, 2015, **C71**, 3-8.
8. Rigaku Oxford Diffraction, *CrysAlisPRO Software System*, version 1.171.40.39a (**2019**), Rigaku Corporation, Oxford, UK.
9. O. V. Dolomanov, L. J. Bourhis, R. J. Gildea, J. A. K. Howard, H. Puschmann, *J. Appl. Cryst.* 2009, **42**, 339-341.
10. L. Falivene, Z. Cao, A. Petta, L. Serra, A. Poater, R. Oliva, V. Scarano and L. Cavallo, *Nat. Chem.*, 2019, **11**, 872-879.
11. (a) H. Clavier and S. P. Nolan, *Chem. Commun.*, 2010, **46**, 841-861. (b) M. L. Y. Riu, W. J. Transue, I. Knopf and C. C. Cummins, *Organometallics*, 2020, **39**, 4187-4190.